

This discussion paper is/has been under review for the journal *Atmospheric Chemistry and Physics (ACP)*. Please refer to the corresponding final paper in *ACP* if available.

# Bromocarbons in the tropical marine boundary layer at the Cape Verde Observatory – measurements and modelling

L. M. O'Brien<sup>1</sup>, N. R. P. Harris<sup>1</sup>, A. D. Robinson<sup>1</sup>, B. Gostlow<sup>1</sup>, N. Warwick<sup>1,2</sup>, X. Yang<sup>1,2</sup>, and J. A. Pyle<sup>1,2</sup>

<sup>1</sup>Centre for Atmospheric Science, Department of Chemistry, University of Cambridge, Lensfield Road, Cambridge, CB2 1EW, UK

<sup>2</sup>Global Composition and Climate Research, National Centre for Atmospheric Science, NCAS-Climate, Cambridge, CB2 1EW, UK

Received: 2 December 2008 – Accepted: 8 December 2008 – Published: 10 February 2009

Correspondence to: L. M. O'Brien (lmo29@cam.ac.uk)

Published by Copernicus Publications on behalf of the European Geosciences Union.

## Bromocarbons in the tropical marine boundary layer

L. M. O'Brien et al.

Title Page

Abstract

Introduction

Conclusions

References

Tables

Figures

◀

▶

◀

▶

Back

Close

Full Screen / Esc

Printer-friendly Version

Interactive Discussion



## Abstract

A new gas chromatograph was used to make measurements of halocarbons at the Cape Verde observatory during late May and early June 2007. The instrument demonstrated its potential for long-term autonomous measurements. Bromoform ( $\text{CHBr}_3$ ) exhibits the most variability of all the halocarbons observed, ranging from a background concentration of about 4 ppt to a maximum of  $>40$  ppt during the course of the measurement period. Dibromomethane ( $\text{CH}_2\text{Br}_2$ ) correlates well with  $\text{CHBr}_3$ , suggesting a common regional source. Methyl iodide ( $\text{CH}_3\text{I}$ ) does not correlate with these bromocarbons, with base levels of around 1–2 ppt and some periods of much higher mixing ratios. Model studies with published bromocarbon emission rates do not reproduce the observations. Local emission magnitudes and  $\text{CHBr}_3:\text{CH}_2\text{Br}_2$  ratios must be increased more in line with the recent observations of Yokouchi et al. (2005) to improve the model to measurement comparison. Even when the model reproduces the observed bromocarbons, modelled BrO is much less than recent tropical observations (Read et al., 2008). A sea salt source seems the likely explanation. When high BrO is reproduced, the model agrees much better with the observed ozone changes, including diurnal variation, during the measurement period but it is suggested that a representation of iodine chemistry in the model is also required.

## 1 Introduction and background

It is widely accepted that reactive halogen compounds, both of natural and anthropogenic origin, play an important role in controlling the composition of the global atmosphere, and so can also influence climate and local air quality. Stratospheric ozone depletion in recent decades has been driven by substantial increases in the atmospheric concentrations of a number of anthropogenic halogen compounds. Thus, both chlorine and bromine species are centrally implicated in the large observed ozone destruction in polar regions, as well as in the downward trends in middle latitude ozone. These

## Bromocarbons in the tropical marine boundary layer

L. M. O'Brien et al.

Title Page

Abstract

Introduction

Conclusions

References

Tables

Figures

◀

▶

◀

▶

Back

Close

Full Screen / Esc

Printer-friendly Version

Interactive Discussion



**Bromocarbons in the  
tropical marine  
boundary layer**

L. M. O'Brien et al.

[Title Page](#)[Abstract](#)[Introduction](#)[Conclusions](#)[References](#)[Tables](#)[Figures](#)[⏪](#)[⏩](#)[◀](#)[▶](#)[Back](#)[Close](#)[Full Screen / Esc](#)[Printer-friendly Version](#)[Interactive Discussion](#)

anthropogenic compounds are now regulated by the Montreal Protocol and their atmospheric abundances have started to decline (see WMO, 2007). However, a number of naturally emitted species are also important for stratospheric ozone chemistry. In particular, it seems that the observed abundance of stratospheric bromine (about 25 ppt) cannot be explained simply by the breakdown in the stratosphere of methyl bromide, which has natural as well as anthropogenic sources, and the halons (the anthropogenic bromine compounds widely used in fire protection). Additional short-lived bromine compounds, mainly of natural origin, are needed to balance the bromine budget in the lower stratosphere (Salawitch, 2006; WMO, 2007). In tropical latitudes, deep convection could potentially lift these halogenated species to the upper troposphere/lower stratosphere (UTLS) region, on time scales shorter than the species' lifetime. Photolysis, or oxidation reactions, would then release the active halogen atoms (bromine, but possibly also chlorine and iodine), which could then contribute to stratospheric ozone depletion.

In contrast to the stratosphere, our understanding of the role of halogens in the global troposphere is still evolving rapidly. It has been clear for some years that brominated compounds are responsible for sporadic, rapid ozone depletion in the polar boundary layer (e.g. Barrie et al., 1988). In the last few years modelling studies by von Glasow et al. (2004) and Yang et al. (2005) have argued that bromine compounds, including both bromocarbons and inorganic salts, can have an important influence on global tropospheric ozone and oxidising capacity. Recent measurements at Cape Verde (Read et al., 2008) show year-round concentrations of reactive BrO and IO of several ppt, sufficient to play an important role in controlling local ozone concentrations.

A number of important, unresolved questions relate to the source of the halogens in both tropospheric and stratospheric chemistry. In particular, we need to understand the source processes, their magnitudes, temporal and spatial distributions and variability. Halocarbons have anthropogenic and natural sources with atmospheric lifetimes varying from days to centuries. While we understand the sources and ultimate fate of long-lived halogenated species (such as the man-made CFCs), shorter-lived compounds

**Bromocarbons in the  
tropical marine  
boundary layer**

L. M. O'Brien et al.

are still poorly understood in terms of their global fluxes and, as a result, their contributions to the tropospheric and stratospheric ozone budgets are also uncertain. Their short lifetimes of typically days and weeks (compared to, for example, many decades for the major CFCs) mean that it is not straightforward to resolve their global budgets, especially if they might be emitted in highly variable amounts globally; there could, for example, be a number of “hot spot” emission regions.

Recently, attention has focused on the naturally emitted bromine- and iodine-containing compounds in particular (for example see von Glasow et al., 2004; Salawitch, 2006; Yokouchi et al., 2005 and Bassford et al., 1999). Short-lived brominated and iodinated halocarbons are known sources of BrO and IO radicals to the atmosphere (Yang et al., 2005); bromine and iodine are more efficient than chlorine at destroying stratospheric ozone (e.g. Chipperfield and Pyle, 1998). Bromoform (CHBr<sub>3</sub>) is the major natural contributor of bromine to the atmosphere (Penkett et al., 1985; Goodwin et al., 1997); it is predominantly oceanic in origin, with tropical macroalgae constituting an important source. An open ocean source, related to phytoplankton, has also been identified (e.g. Butler et al., 2007). Other important biogenic compounds of marine origin include dibromomethane (CH<sub>2</sub>Br<sub>2</sub>), dibromochloromethane (CHBr<sub>2</sub>Cl) and iodine-containing species such as methyl iodide (CH<sub>3</sub>I). Carpenter and Liss (2000) provide an extensive list of red, green and brown algae, which have been suggested as sources of halocarbons for the atmosphere. Important macroalgae species identified as potentially important sources of CHBr<sub>3</sub> (and perhaps other brominated species and CH<sub>3</sub>I) by Moore and Tokarczyk (1993) include *Ascophyllum nodosum* (with *Elachista fuciculosa* growing as an epiphyte) and *Fucus vesiculosus*. They suggested (see also Norton and Mathieson, 1983) that free-floating algae provide a source of halogenated compounds such as CHBr<sub>3</sub>. *Fucales sargassum* and *Laminariae laminariales* were two species of brown algae investigated by Class and Ballschmiter (1988); the main compounds associated with the former were CH<sub>2</sub>Br<sub>2</sub>, CHBr<sub>3</sub>, CHBr<sub>2</sub>Cl, CHBrCl<sub>2</sub> and CH<sub>2</sub>I<sub>2</sub>. While macroalgae have been identified as an important direct source for the various bromochloromethanes, halogen-exchange reac-

[Title Page](#)[Abstract](#)[Introduction](#)[Conclusions](#)[References](#)[Tables](#)[Figures](#)[◀](#)[▶](#)[◀](#)[▶](#)[Back](#)[Close](#)[Full Screen / Esc](#)[Printer-friendly Version](#)[Interactive Discussion](#)

tions, e.g.  $\text{CHBr}_3 + \text{Cl}^- \rightarrow \text{CHBr}_2\text{Cl} + \text{Br}^-$ , may constitute a secondary source for certain species (Class and Ballschmiter, 1988). In addition to the bromocarbons, sea salt is an extremely important source of bromine, especially to the marine boundary layer (Yang et al., 2005).

Iodine compounds are thought to have a different marine source to the chlorinated and brominated species; Ekdahl et al. (1998) reported that photosynthesis, respiration and photorespiration were important sources of the latter. *Laminaria digitata* is an Atlantic giant kelp species which has a very large iodine content and is thus recognised as an important source of  $\text{CH}_3\text{I}$  (e.g. Grose et al., 2007). Like  $\text{CHBr}_3$ ,  $\text{CH}_3\text{I}$  may also be emitted in the open ocean from phytoplankton (e.g. diatoms, dinoflagellates, chlorophytes, coccolithophores and *Phaeocystis* sp.); such a source provides a smaller flux rate than from macroalgae, but a significant global flux owing to the large area of open ocean (Grose et al., 2007).

Many of the major and minor sources of atmospheric chlorine are man-made, including the CFCs,  $\text{CCl}_4$ ,  $\text{CH}_3\text{CCl}_3$  and  $\text{C}_2\text{Cl}_4$ .  $\text{CH}_3\text{Cl}$  has important natural sources (WMO, 2007). Chloroform ( $\text{CHCl}_3$ ) may be produced both naturally (pine forests and peat bogs (Carpenter et al., 2005), soils (Hoekstra et al., 1998) and oceans (Khalil et al., 1999; Rivett et al., 2003)) and anthropogenically.

The short-lived biogenic halocarbons have been measured in very variable concentrations in a number of different locations, emphasizing the importance of localized emissions of these compounds, which show both temporal and spatial variability. With a lifetime with respect to photolysis and reaction with hydroxyl (OH) radicals of two to three weeks (Warwick et al., 2006),  $\text{CHBr}_3$  exhibits large spatial variability. For example, a study by Carpenter et al. (2007) measured  $\text{CHBr}_3$  concentrations over the eastern Atlantic Ocean between  $25^\circ\text{N}$  and  $25^\circ\text{S}$ , ranging from a minimum of 0.2 ppt to a maximum of 13.3 ppt at  $9.5^\circ\text{N}$ . Similar maximum mixing ratios of  $\text{CHBr}_3$  over the tropical northern Atlantic Ocean were observed by Class and Ballschmiter (1988) (14 ppt) and Quack et al. (2004) (25 ppt). In the eastern Atlantic Ocean, the bioactive Mauritanian upwelling has been suggested as an important source of reactive organic bromine

## Bromocarbons in the tropical marine boundary layer

L. M. O'Brien et al.

Title Page

Abstract

Introduction

Conclusions

References

Tables

Figures

◀

▶

◀

▶

Back

Close

Full Screen / Esc

Printer-friendly Version

Interactive Discussion



**Bromocarbons in the  
tropical marine  
boundary layer**

L. M. O'Brien et al.

Title Page

Abstract

Introduction

Conclusions

References

Tables

Figures

◀

▶

◀

▶

Back

Close

Full Screen / Esc

Printer-friendly Version

Interactive Discussion



(Quack et al., 2007; Carpenter et al., 2007), though ship-borne measurements taken in May/June 2008 found no instances of high  $\text{CH}_2\text{Br}_2$  or  $\text{CHBr}_3$  concentrations (Carpenter et al., 2008). Ekdahl et al. (1998) presented extremely high atmospheric concentrations of  $\text{CHBr}_3$  from a rock pool (with no tidal influences during sampling) of volume  $10\text{ m}^3$  on the island of Gran Canaria in the Atlantic Ocean (2000–26 000 ppt range). High concentrations of other halogenated species were also measured during this study (e.g.  $\text{CH}_2\text{Br}_2$  (37–340 ppt),  $\text{CH}_3\text{I}$  (24–84 ppt) and  $\text{CHBr}_2\text{Cl}$  (19 to 130 ppt)). Biogenic compounds have also been measured in a variety of locations around the globe, although the coverage is still rather sparse in terms of the global area.

Shallow coastal areas seem to be particularly important for emissions of oceanic halocarbons. Yokouchi et al. (2005) observed a maximum of 40 ppt of  $\text{CHBr}_3$  at the coast on San Cristobal Island in the tropical Pacific Ocean, with similar concentrations being measured at a coastal site on Christmas Island, also in the tropical Pacific Ocean. The highest concentrations of polybromomethanes coincided with the onshore sea breeze, across the coastal zone. Several studies have also shown  $\text{CHBr}_3$  and  $\text{CH}_2\text{Br}_2$  to be well correlated in coastal locations, suggesting a common source for these compounds (for example see Quack et al., 2007; Yokouchi et al., 2005). Yokouchi et al. (2005) found that correlations amongst these compounds were weak or absent for open ocean samples over the Pacific Ocean, as well as for an inland site on Java Island; concentrations were also much lower than those for coastal sites. Air samples taken along the coastlines of islands (Bermuda, Sao Miguel and Tenerife) by Class and Ballschmiter (1988) revealed concentrations of up to 200 ppt for  $\text{CHBr}_3$  and 25 ppt for  $\text{CH}_2\text{Br}_2$ .

Global emission magnitudes and distributions for the short-lived oceanic bromocarbons are not well constrained due to their high geographical and temporal variability. Emission estimates for  $\text{CHBr}_3$  are particularly uncertain and estimates from a variety of studies range from  $200\text{ Gg Br yr}^{-1}$  to over  $1000\text{ Gg Br yr}^{-1}$ . Global emissions for the other oceanic bromocarbons are less well studied. WMO (2003) recommended emission values for  $\text{CHBr}_3$ ,  $\text{CH}_2\text{Br}_2$  and  $\text{CHBr}_2\text{Cl}$  of 209, 61 and  $8\text{ Gg Br yr}^{-1}$  respec-

**Bromocarbons in the  
tropical marine  
boundary layer**

L. M. O'Brien et al.

Title Page

Abstract

Introduction

Conclusions

References

Tables

Figures

◀

▶

◀

▶

Back

Close

Full Screen / Esc

Printer-friendly Version

Interactive Discussion

tively, based on estimates of global burdens and local lifetimes (calculated using an OH concentration of  $1 \times 10^6$  molec  $\text{cm}^{-3}$  and a globally and seasonally averaged photolysis constant). The more detailed 3-D model study by Warwick et al. (2006) assumed that emissions of these compounds were predominantly situated in the tropics. They therefore calculated lower global lifetimes due to higher OH concentrations and solar radiation in this region, requiring higher emissions to reproduce atmospheric observations. The Warwick et al. (2006) emission estimates for  $\text{CHBr}_3$ ,  $\text{CH}_2\text{Br}_2$  and  $\text{CHBr}_2\text{Cl}$  were 565, 104 and 18 Gg  $\text{Br yr}^{-1}$  respectively, significantly larger than the WMO (2003) estimates. Bottom-up studies based on global extrapolations of local fluxes also produced relatively high global emission estimates of 780 and 800 Gg  $\text{Br yr}^{-1}$  for  $\text{CHBr}_3$  and 280 Gg  $\text{Br yr}^{-1}$  for  $\text{CH}_2\text{Br}_2$  (Quack and Wallace, 2003; Butler et al., 2007). Yokouchi et al. (2005) calculated a  $\text{CHBr}_3:\text{CH}_2\text{Br}_2:\text{CHBr}_2\text{Cl}$  emission ratio of 9:1:0.7 and obtained global emission estimates for  $\text{CHBr}_3$  and  $\text{CHBr}_2\text{Cl}$  of 820 and 43 Gg  $\text{Br yr}^{-1}$ , using the relatively low WMO (2003)  $\text{CH}_2\text{Br}_2$  emission value.

In this work, we report measurements made at the Cape Verde Atmospheric Observatory by  $\mu$ -Dirac, our gas chromatograph with electron capture detector (GC-ECD).  $\mu$ -Dirac is the latest version (Gostlow et al., 2009) of the Dirac instrument, which measures a range of halocarbons (Robinson et al., 2000, 2005). The new version is purpose-built and relatively inexpensive, being designed to make long-term measurements of a small number of halocarbons. Its relatively low cost and ease of operation mean that the instrument can be deployed at a number of surface sites, thereby providing a valuable constraint on variability and emission estimates. Two instruments were deployed at Cape Verde in May and June 2007, during an intensive field campaign. They were optimised for the measurement of a number of the short-lived compounds mentioned above, allowing measurements of  $\text{CHBr}_3$ ,  $\text{CH}_2\text{Br}_2$ ,  $\text{CHBr}_2\text{Cl}$ ,  $\text{CH}_3\text{I}$  and  $\text{C}_2\text{Cl}_4$ , plus a number of longer-lived species. Our objectives here are threefold: to present the measurement series; to explore the implications for emissions and to investigate the role of the measured compounds in controlling local oxidizing capacity. In Sect. 2 we introduce the experimental and modelling tools used, followed in Sect. 3



by a discussion of the prevailing meteorological conditions. The Cape Verde ground-based measurements are presented in Sect. 4.1. Model results are shown in Sect. 4.2 with further exploration of the data in Sect. 4.3. Conclusions and outlook for further work are presented in Sect. 5.

## 2 Experimental details

### 2.1 The Cape Verde Observatory

The Cape Verde Atmospheric Observatory is a recently established monitoring site, situated at 16.8° N, 24.9° W on the island of Sao Vicente, Cape Verde. It is an ideal site for sampling “background” air within the tropical marine boundary layer. A 3-week intensive field campaign, part of the NERC SOLAS/RhaMbLe project, took place in May/June 2007 in and around Cape Verde (see Read et al., 2008). A large range of ground-based, aircraft and ship-borne instruments were deployed, to complement the long-term measurements that have been established at the observatory (<http://www.york.ac.uk/capeverde/>). Using  $\mu$ -Dirac, gas chromatographic measurements of a variety of halocarbons with a range of lifetimes and sources were made at the observatory during the 3-week intensive. These were complemented by a set of  $\mu$ -Dirac aircraft measurements made on board the NERC ARSF Dornier 228-101 research aircraft, which made a number of flights in the tropical marine boundary layer and lower troposphere of the surrounding area. Only the ground-based measurements are dealt with in this paper (see the BADC website for the Dornier data; <http://badc.nerc.ac.uk/data/solas/>).

### 2.2 The $\mu$ -Dirac gas chromatograph

$\mu$ -Dirac is a custom-built GC-ECD, which makes in situ measurements of halocarbons (Gostlow et al., 2009). It was originally designed for flights on long duration balloons

## Bromocarbons in the tropical marine boundary layer

L. M. O'Brien et al.

Title Page

Abstract

Introduction

Conclusions

References

Tables

Figures

◀

▶

◀

▶

Back

Close

Full Screen / Esc

Printer-friendly Version

Interactive Discussion



**Bromocarbons in the tropical marine boundary layer**

L. M. O'Brien et al.

and so is lightweight and able to operate autonomously for several weeks. Earlier versions have been deployed on balloons, at ground-based sites and on aircraft (Robinson et al., 2000; 2005; Ross et al., 2004).  $\mu$ -Dirac is well suited for long periods of unattended operation. It has a modular design with an adsorbent-containing micro-trap, which removes the halocarbons from the air. A fixed volume of 20 scc is collected for each atmospheric sample. The micro-trap is then flash heated and the desorbed halocarbons are passed through a chromatographic column with temperature and flow programming capability. After temporal separation in the column the flow passes through the ECD, which is extremely sensitive to halocarbons. Instrument control and data collection are achieved using an on-board microcontroller.

During the Cape Verde deployment, the instrument was housed in an air-conditioned container, with the inlet being fixed to the outside at a height of approximately 10 m. The run cycle was roughly 14 min, with a blank sample and a calibration standard being sampled on average after ten atmospheric samples (i.e. every 2 to 3 h). Internal instrument cooling is achieved using Peltier coolers. The species that are measured include: CFC-11, CFC-113,  $\text{CH}_3\text{CCl}_3$ ,  $\text{CCl}_4$ ,  $\text{CH}_3\text{I}$ ,  $\text{CHCl}_3$ ,  $\text{CHBr}_2\text{Cl}$ ,  $\text{CHBrCl}_2/\text{CH}_2\text{Br}_2$ ,  $\text{C}_2\text{Cl}_4$ , and  $\text{CHBr}_3$ . In this paper we report results for  $\text{C}_2\text{Cl}_4$ ,  $\text{CHCl}_3$ ,  $\text{CH}_3\text{I}$ ,  $\text{CH}_2\text{Br}_2$ ,  $\text{CHBr}_2\text{Cl}$  and  $\text{CHBr}_3$ . Their measurement characteristics are given in Table 1.

The absolute calibration for most of the reported gases is determined by reference to the NOAA-ESRL calibration standard, with an on-board standard gas bottle being filled directly with air from the NOAA-ESRL standard. The one exception is  $\text{CHBr}_2\text{Cl}$ , which is discussed below. The on-board standard lasted for the duration of the campaign. 20 scc samples of the NOAA-ESRL calibration standard gas were measured every 2 to 3 h assuring a direct link to that scale. Calibration between groups is an important issue and there are discrepancies between our measurements and preliminary measurements made during the campaign at the same site by the University of Bristol (S. O'Doherty, personal communication). The  $\mu$ -Dirac measurements of, for example,  $\text{CH}_3\text{CCl}_3$  are in agreement with concurrent measurements from the NOAA-ESRL and AGAGE networks, indicating that any problems are related to specific gases. We are

[Title Page](#)[Abstract](#)[Introduction](#)[Conclusions](#)[References](#)[Tables](#)[Figures](#)[◀](#)[▶](#)[◀](#)[▶](#)[Back](#)[Close](#)[Full Screen / Esc](#)[Printer-friendly Version](#)[Interactive Discussion](#)

taking part in an international comparison of VSLH calibration scales performed within the SOLAS/IGAC initiative HiT.

No calibration standard for  $\text{CHBr}_2\text{Cl}$  was available during this deployment, although it was detectable in the NOAA-ESRL calibration gas. Here we use the ratio of this peak to that of  $\text{CH}_2\text{Br}_2$  in the calibration gas to estimate the calibration concentration. The ECD responses for the molecules are dominated by the two bromine atoms, suggesting similar sensitivities for the two species. In this case, the ratio of the calibration signals would be the same as the ratio of the concentrations in the calibration gas. With 4.8 ppt of  $\text{CH}_2\text{Br}_2$  in the calibration gas, we estimate that the standard contained 0.19 ppt of  $\text{CHBr}_2\text{Cl}$ . Clearly, the absolute accuracy of our determination of  $\text{CHBr}_2\text{Cl}$  is low and we estimate this as 50% in Table 1. However the precision is relatively good (9.6%, see Table 1) and it is thus safe to investigate its variability during the measurement period and its correlation with other species.

The peaks for  $\text{CHBrCl}_2$  and  $\text{CH}_2\text{Br}_2$  currently overlap, each having a retention time of about 5.1 min. Careful examination of a subset of chromatograms taken in Cape Verde suggests that  $\text{CHBrCl}_2$  was present only in small quantities. However, for the majority of our chromatograms, it was not possible to resolve the two peaks, owing to their nearly identical retention times. The ECD response depends on the electron-capture coefficient, which represents the degree to which the compound is able to capture thermal electrons (see, e.g., Lovelock, 1961; Dessler, 1986). Halogenated compounds produce one of the highest responses in an ECD, with the structure of the compound being particularly important in determining the ECD sensitivity. Iodine produces the greatest ECD response, followed by Br, then Cl and finally F. The electron-capture coefficients ( $K$ ) are  $9 \times 10^4$  for I,  $3 \times 10^2$  for Br, 1 for Cl and  $\ll 1$  for F (Pellizzari, 1974). In addition, the number of halogen atoms on a carbon atom is important (i.e. whether we are dealing with tetra-, tri-, di- or mono- compounds; relative values of  $4 \times 10^5$ ,  $6 \times 10^4$ ,  $10^2$  and 1, respectively). Based on this information, it is likely that the ECD is significantly more sensitive to  $\text{CH}_2\text{Br}_2$  than to  $\text{CHBrCl}_2$ . Furthermore, atmospheric  $\text{CHBrCl}_2$  concentrations are usually less than those of  $\text{CH}_2\text{Br}_2$ ; Schall et al. (1997) concluded

## Bromocarbons in the tropical marine boundary layer

L. M. O'Brien et al.

Title Page

Abstract

Introduction

Conclusions

References

Tables

Figures

◀

▶

◀

▶

Back

Close

Full Screen / Esc

Printer-friendly Version

Interactive Discussion



that the typical order is  $[\text{CHBr}_3] > [\text{CH}_2\text{Br}_2] > [\text{CHBr}_2\text{Cl}] > [\text{CHBrCl}_2]$ . In summary, for reasons of chromatographic sensitivity and expected atmospheric abundances, we report the combined peak ( $[\text{CH}_2\text{Br}_2] + [\text{CHBrCl}_2]$ ) as simply  $[\text{CH}_2\text{Br}_2]$ .

### 2.3 The model

5 For our modelling studies we have used the global chemistry and transport model p-TOMCAT (see Law et al., 2000; Savage et al., 2004). Here we base the model on a version of p-TOMCAT described by Yang et al. (2005) which includes a detailed description of tropospheric bromine chemistry, including emissions of bromocarbons ( $\text{CH}_3\text{Br}$ ,  $\text{CHBr}_3$ ,  $\text{CH}_2\text{Br}_2$ ,  $\text{CH}_2\text{BrCl}$ ,  $\text{CHBr}_2\text{Cl}$  and  $\text{CHBrCl}_2$ ) from Warwick et al. (2006) and a treatment of the inorganic sea salt source from the open ocean. The bromine chemistry scheme contains both gas-phase reactions and heterogeneous reactions on cloud particles and background aerosols. A total of 13 bromine-containing compounds are considered in the model: 7 inorganic compounds ( $\text{Br}$ ,  $\text{Br}_2$ ,  $\text{BrO}$ ,  $\text{HOBr}$ ,  $\text{BrONO}_2$ ,  $\text{BrNO}_2$  and  $\text{HBr}$ ) and the 6 emitted organic compounds. Here, the model is improved (see Yang et al., 2008a) by considering a size dependent bromine depletion factor to describe the bromine release from sea salt aerosols (rather than the constant value used in our earlier study), as well as a third atmospheric bromine source coming from blowing snow on sea ice (although the latter, of course, has modest immediate impact in the tropics). The bromine chemistry scheme has also been updated by adding 3 further heterogeneous reactions to reactivate inactive gaseous species, including  $\text{HBr}$ , to active forms, such as  $\text{BrO}$  (Yang et al., 2008b). The model does not include a scheme for active iodine chemistry. However, in order to compare with our observations, surface emissions of  $\text{CH}_3\text{I}$  and loss via photolysis and reaction with  $\text{OH}$  have been added.

25 Emission datasets for the oceanic bromocarbons are from Warwick et al. (2006), Scenario B. The geographical distribution consists of a band of emissions in the tropical open ocean, with bands of weaker emissions in northern and southern mid-latitudes. For  $\text{CHBr}_3$ , the dataset also includes increased emissions along tropical coastlines. These emissions are aseasonal.

## Bromocarbons in the tropical marine boundary layer

L. M. O'Brien et al.

Title Page

Abstract

Introduction

Conclusions

References

Tables

Figures

◀

▶

◀

▶

Back

Close

Full Screen / Esc

Printer-friendly Version

Interactive Discussion



---

**Bromocarbons in the  
tropical marine  
boundary layer**L. M. O'Brien et al.

---

In this study, p-TOMCAT was run with a  $2.8^{\circ} \times 2.8^{\circ}$  horizontal resolution, with 31 vertical levels from the surface to 10 hPa. The offline meteorological fields used are from the European Medium Range Weather Forecast reanalysis data, updated every 6 h. We focus here on a period from late May to mid June 2007. All the runs performed are based on a spun-up integration which covers this period. For descriptions of other physical parameterisations see Cook et al. (2007).

### 3 Overview of meteorological conditions

For the duration of the measurement period, the Cape Verde islands were generally under the influence of a region of Atlantic high pressure. Typically, the mean sea level pressure at the site was fairly constant at around 1015 mb. The  $\mu$ -Dirac measurement period lasted from 30 May 2007 until 15 June 2007 (with a few short breaks in the data due to technical problems at the site). At the start of the campaign, there was a large high pressure area situated over the central Atlantic Ocean, to the north of the archipelago. This was the dominant system over the northern Atlantic Ocean, with some smaller low pressure areas further north towards Ireland, and also over the Mali/Niger region of West Africa. Throughout the course of the next couple of days the large region of high pressure over the mid north-Atlantic gradually moved further north-east, eventually splitting into two separate high pressure regions extending from the French and Spanish mainland out to the Atlantic Ocean off the Portuguese coast. Further high pressure areas developed to replace the earlier northward moving systems. The area of low pressure over the West African mainland had moved northwards over Morocco/Algeria by 5 June 2007, with a smaller area of low pressure also present over the open Atlantic Ocean to the west of Portugal. By the evening of 6 June 2007, weak cyclonic conditions had developed around this Atlantic low pressure region, persisting for a couple of days until 9 June 2007, when it was replaced by a south-easterly moving area of high pressure, which originated to the west of the low. The cyclonic conditions continued to persist as the low pressure moved further north by 10 June 2007, but the

[Title Page](#)[Abstract](#)[Introduction](#)[Conclusions](#)[References](#)[Tables](#)[Figures](#)[◀](#)[▶](#)[◀](#)[▶](#)[Back](#)[Close](#)[Full Screen / Esc](#)[Printer-friendly Version](#)[Interactive Discussion](#)

Cape Verde islands once again came under the influence of a large mid-Atlantic high pressure region. This situation remained until the end of the measurement period.

The measurement site was characterised by a very stable boundary layer, whose depth of about 1000 m was roughly constant during the course of the campaign (but see Sect. 4.2). A strong temperature inversion of up to 10°C separated this marine boundary layer from the free troposphere above. Local wind speeds ranged from about 2 ms<sup>-1</sup> to 12 ms<sup>-1</sup> over the measurement period. The wind direction ranged from about 10 to 80°; generally it was about 50° (i.e. dominated by north-easterlies). A period of generally decreasing wind speeds was observed from 5 June to 8 June 2007, with wind speeds reaching a minimum of about 2 ms<sup>-1</sup> by 8 June 2007. Wind speeds then increased generally during 9 and 10 June 2007. The wind speeds reached a maximum during the day. (See <http://www.york.ac.uk/capeverde/>).

Figure 1 shows typical trajectories obtained from the British Atmospheric Data Centre (<http://badc.nerc.ac.uk/home/index.html>), arriving at 950 hPa at Cape Verde on 25 May and 5, 7 and 15 June 2007. All the trajectories are characterised by flow around the Azores anticyclone. For 25 May 2007, the air parcels have travelled predominantly over the ocean, while for 5 June 2007 they have spent time over Spain and Portugal. For 7 June 2007, the north easterly flow crossed closer to coastal regions of the Iberian Peninsula, West Africa and the Canary Islands. For 15 June 2007, air parcels travel along the West African coast. In all cases, the air parcels spent time in the boundary layer prior to arrival at Cape Verde.

## 4 Results

### 4.1 Observations from the Cape Verde Observatory

Figure 2 presents the concentration time series for the period from late May until 15 June 2007 at the end of the campaign. Measurements for CHBr<sub>3</sub>, CH<sub>3</sub>I, CH<sub>2</sub>Br<sub>2</sub>, CHBr<sub>2</sub>Cl, CHCl<sub>3</sub> and C<sub>2</sub>Cl<sub>4</sub> are shown. This data is also summarised in Table 2, which

## Bromocarbons in the tropical marine boundary layer

L. M. O'Brien et al.

Title Page

Abstract

Introduction

Conclusions

References

Tables

Figures

◀

▶

◀

▶

Back

Close

Full Screen / Esc

Printer-friendly Version

Interactive Discussion



shows average, mean, median, maximum and minimum mixing ratios for each of the halocarbons for each day of the measurement period. Note that the periods of missing data are due to power cuts at the observatory.

There is a strong correlation between  $\text{CHCl}_3$  and  $\text{C}_2\text{Cl}_4$ . Figure 3 plots these two species alongside the CO measurements from the observatory (<http://www.york.ac.uk/capeverde/>). All three species correlate well. High mixing ratios are seen on 5 and 6 June 2007 when the trajectories indicate that the air has previously crossed over Spain and Portugal. On shorter time scales note the decrease in all species late on 9 June 2007. It is clear that, like CO,  $\text{CHCl}_3$  and  $\text{C}_2\text{Cl}_4$  are largely anthropogenic.  $\text{C}_2\text{Cl}_4$  is believed to be an exclusively industrial compound and serves as a useful tracer of anthropogenic activity;  $\text{CHCl}_3$  has both natural and anthropogenic sources. The increases here seem to relate principally to the latter.  $\text{C}_2\text{Cl}_4$  mixing ratios are very low at a few parts per trillion, typical of relatively unpolluted background air which has not been influenced by any major local industrial sources. The other, longer-lived anthropogenic halocarbons ( $\text{CCl}_4$ ,  $\text{CFCl}_3$ ,  $\text{CH}_3\text{CCl}_3$ , not shown) show little variability during the measurement period.

Bromoform ( $\text{CHBr}_3$ ) exhibits the most variability of all the halocarbons observed, ranging from a background concentration of about 4 ppt to a maximum of >40 ppt during the course of the measurement period. As discussed in Sect. 1, coastal sites are thought to be important sources of  $\text{CHBr}_3$ , and in the tropical eastern Atlantic region where the Cape Verde islands are situated, the Mauritanian upwelling (north-west African coast) is also thought to be an important halocarbon source region (Quack et al., 2007; Carpenter et al., 2007). Two important factors which drive this upwelling are the persistent north-easterly trade winds and the seasonally variable Canary Current, an eastern boundary current flowing from north to south along the north-west African coast. Its surface waters are relatively cool because as it travels south it entrains upwelled water from the coast. Various studies have reported maximum chlorophyll A (Chl-*a*) concentrations to occur in late spring/early summer in the region of the Mauritanian upwelling (Pradhan et al., 2006; Thomas et al., 2001).

---

**Bromocarbons in the tropical marine boundary layer**L. M. O'Brien et al.

---

[Title Page](#)[Abstract](#)[Introduction](#)[Conclusions](#)[References](#)[Tables](#)[Figures](#)[◀](#)[▶](#)[◀](#)[▶](#)[Back](#)[Close](#)[Full Screen / Esc](#)[Printer-friendly Version](#)[Interactive Discussion](#)

**Bromocarbons in the  
tropical marine  
boundary layer**

L. M. O'Brien et al.

Title Page

Abstract

Introduction

Conclusions

References

Tables

Figures

◀

▶

◀

▶

Back

Close

Full Screen / Esc

Printer-friendly Version

Interactive Discussion

The time period of our measurement campaign coincides with these reported periods of maximum primary productivity in the upwelling region. SeaWiFS data for June 2007 (<http://oceancolor.gsfc.nasa.gov/SeaWiFS/>) show maximum CHL-*a* along the West African coast, extending into the ocean around the Mauritanian upwelling.

Coincidence between these regions and the back trajectories is consistent with the hypothesis that high halocarbon concentrations are related to these regions of high productivity.

Two very large  $\text{CHBr}_3$  peaks, corresponding to the maximum  $\text{CHBr}_3$  observed during the campaign ( $>40$  ppt), occurred during a period of elevated  $\text{CHBr}_3$  concentrations between 7–10 June 2007. Maximum  $\text{CHBr}_3$  mixing ratios were observed at approximately midday on both 7 and 8 June 2007. Meanwhile, during this period mixing ratios of the anthropogenic species ( $\text{CHCl}_3$ ,  $\text{C}_2\text{Cl}_4$  and CO) were some of the lowest observed during the whole campaign (Fig. 3). The very high concentrations and the large amount of scatter in the  $\text{CHBr}_3$  data suggest that there is a regional tropical source around the islands contributing to the measurements. For example, the site was directly exposed to the local north-easterly trade winds, which may have transported high levels of  $\text{CHBr}_3$  from local oceanic sources to the site.

Figure 4 plots the two-hour running mean of the measured  $\text{CHBr}_3$  alongside the surface ozone measurements from the observatory. During the period with elevated  $\text{CHBr}_3$ , the ozone concentration declines by about 10 ppb and shows a clearly defined diurnal variation. We will discuss these observations in Sect. 4.2.

Figure 2 clearly shows a good correlation between  $\text{CHBr}_2\text{Cl}$  and  $\text{CHBr}_3$ , and  $\text{CH}_2\text{Br}_2$  also correlates well with  $\text{CHBr}_3$  (see Sect. 4.3). Mixing ratios of  $\text{CH}_3\text{I}$  are generally 1 or 2 ppt, but higher peaks in concentration occur on 10, 11 and 15 June 2007. The increased concentrations on 10 and 11 June 2007 do not correlate well with  $\text{CHBr}_3$ , suggesting a different source. Many of the species, with both anthropogenic and natural sources, show very high concentrations on 15 June 2007. This was the day chosen ahead of time to end the period of autonomous measurement in order to return the instrument to Cambridge, so unfortunately we are unable to say for how long these

high concentrations were sustained. Nevertheless, Fig. 1 suggests that the air masses sampled at Cape Verde may have passed previously over the Canary Islands as well as biologically productive coastal regions.

#### 4.2 Modelling results and comparison with the observations

5 We have used the p-TOMCAT chemical transport model to address three broad questions:

- Are the observed halocarbon measurements, presented above, consistent with proposed emissions and, if not, what emission distribution is required?
- Are the bromine sources, based on our observed halocarbons and modelled sea salt emissions, consistent with observed BrO at Cape Verde of around 2–3 ppt (Read et al., 2008)?
- Can we model the observed diurnal changes in ozone shown in Fig. 4?

10 We have performed a number of calculations with p-TOMCAT. These include a run without bromine chemistry (NoBr); a base run (MON) with a halocarbon emission distribution based on Warwick et al. (2006) and using the Monahan et al. (1986) sea salt source, as presented previously by Yang et al. (2005); a run with elevated bromocarbon emissions across the region from 10–20° N and 20–30° W (HiBr), covering several model grid boxes surrounding Cape Verde; a run using the same emissions as HiBr but without the sea salt source (Org). Finally, HiSALT includes a substantial increase in sea salt bromine over the same region.

15 We have compared the measured halocarbons at Cape Verde with model results for the same period. In MON the model significantly underestimates the observed concentrations (not shown). The emissions chosen from Warwick et al. (2006) (emission scenario B from that paper) peak along tropical coast lines; modelled emissions at Cape Verde (representative of the open ocean) are lower, with these emissions uniformly distributed from 20° N to 20° S. Thus the model has no representation of potential

## Bromocarbons in the tropical marine boundary layer

L. M. O'Brien et al.

Title Page

Abstract

Introduction

Conclusions

References

Tables

Figures



Back

Close

Full Screen / Esc

Printer-friendly Version

Interactive Discussion



emission “hot spots” such as the Mauritanian upwelling. In an attempt to reproduce the observations we have rather arbitrarily scaled up the 24-h mean emissions of  $\text{CHBr}_3$  and  $\text{CH}_2\text{Br}_2$  by factors 10 and 2.5 over a region from 10–20° N and 20–30° W. Model results from this run are shown in Fig. 5 (where the enhanced emissions in  $\text{HiBr}$  were included only during the daytime). Total emissions in this region increased from 1.4 to 14  $\text{Gg Br yr}^{-1}$  for  $\text{CHBr}_3$  and from 0.52 to 1.31  $\text{Gg Br yr}^{-1}$  for  $\text{CH}_2\text{Br}_2$  using these multiplication factors. The increased emissions correspond to an ocean-atmosphere flux of 80  $\text{nmol m}^{-2} \text{ day}^{-1}$  (or 14  $\text{Gg Br yr}^{-1}$ ) for  $\text{CHBr}_3$  in the selected region, which is within the (very wide) range of fluxes calculated from coastal surface air and water  $\text{CHBr}_3$  concentrations around the globe in Butler et al. (2007) and Quack and Wallace (2003). Total global emissions increased from 565  $\text{Gg Br yr}^{-1}$  to 578  $\text{Gg Br yr}^{-1}$  for  $\text{CHBr}_3$  and from 104 to 105  $\text{Gg Br yr}^{-1}$  for  $\text{CH}_2\text{Br}_2$ . For  $\text{CH}_3\text{I}$  we assumed a distribution of emissions similar to that of  $\text{CHBr}_3$ , with an ocean-atmosphere flux of 57  $\text{nmol m}^{-2} \text{ day}^{-1}$ . With these increases in emissions the modelled concentrations of  $\text{CH}_2\text{Br}_2$  and  $\text{CH}_3\text{I}$  are similar in magnitude to the observations and some of the structure is reproduced (see below). However, modelled  $\text{CHBr}_3$  is still about half that observed. Despite the lower concentrations compared with the observations, it is interesting that the model reproduces an increase in  $\text{CHBr}_3$  around 7–10 June 2007. Winds in the surface model layer (and in the atmosphere) were very low at this time and the increase reflects a stable, confined boundary layer. We have already noted in Sect. 4.1 that the trajectories for this period spent several days below about 1 km and passed close to regions with high potential for biological productivity, as indicated by observations from the SeaWiFS satellite.

We could have increased the emissions of  $\text{CHBr}_3$  still further in an attempt to reproduce the observations around 7 and 8 June 2007. However, the observations could also be consistent with a more localised source of  $\text{CHBr}_3$  closer to Cape Verde. Notice that the observations have a diurnal variation, especially around 7–10 June 2007, with peak concentrations in the early afternoon. Bromoform ( $\text{CHBr}_3$ ) has a lifetime in the tropics of 2 weeks or so, and it is difficult to imagine that the diurnal variation is

**Bromocarbons in the tropical marine boundary layer**

L. M. O'Brien et al.

Title Page

Abstract

Introduction

Conclusions

References

Tables

Figures

◀

▶

◀

▶

Back

Close

Full Screen / Esc

Printer-friendly Version

Interactive Discussion



photochemically driven. A more likely possibility is that local marine sources have a diurnal variation (Quack and Wallace, 2003) and that the  $\text{CHBr}_3$  is being sampled soon enough after emission for neither mixing nor atmospheric chemistry to remove the diurnal structure. As stated above, the additional regional emissions for the run shown in Fig. 5 were applied only during the daytime and do suggest a diurnal behaviour (e.g. on 10 and 11 June 2007), while a run with the same emissions, spread across 24 h, does not.

Figure 6 shows the modelled BrO at Cape Verde for the period in early June 2007. None of the model runs discussed above come near to reproducing the average BrO reported by Read et al. (2008) of between 2 and 3 ppt. For example, the run with elevated bromocarbon emissions close to Cape Verde (HiBr) produces only a low BrO level of  $\sim 0.3$  ppt at noon. The bromocarbons included in the model are the major known natural organic sources of bromine. With lifetimes ranging from weeks to months, their high local concentrations do not lead to simultaneously high local concentrations of the radical species. It is possible that very short-lived bromocarbons could be playing a role. A very important known source of reactive bromine to the lowermost troposphere is sea salt (Yang et al., 2005). Wind stress at the ocean surface lifts droplets which evaporate and form sea salt aerosol particles, which can subsequently liberate bromine into the atmosphere. The flux of particles is a strong function of surface wind speed. At the model resolution of approximately  $3^\circ \times 3^\circ$ , low wind speeds are found close to Cape Verde at this time, and sea salt aerosols from the open ocean make almost no contribution to modelled BrO (Fig. 6).

We can arbitrarily increase the modelled sea salt emission to reproduce the observed  $\sim 3$  ppt of BrO. In this case an order of magnitude higher bromine flux of  $0.4 \times 10^{-12} \text{ kg m}^{-2} \text{ s}^{-1}$ , in the form of  $\text{Br}_2$ , must be used. Because of our focus on Cape Verde, and to avoid altering the oxidising capacity of the global atmosphere, emissions were only increased between  $10\text{--}20^\circ \text{ N}$ ,  $20\text{--}30^\circ \text{ W}$ . This high Br flux corresponds to a wind speed of  $13 \text{ ms}^{-1}$  in our sea salt production calculation (based on the Monahan et al. (1986) flux parameterisation). Note that this flux is more than 10 times higher

---

**Bromocarbons in the tropical marine boundary layer**L. M. O'Brien et al.

---

[Title Page](#)[Abstract](#)[Introduction](#)[Conclusions](#)[References](#)[Tables](#)[Figures](#)[⏪](#)[⏩](#)[◀](#)[▶](#)[Back](#)[Close](#)[Full Screen / Esc](#)[Printer-friendly Version](#)[Interactive Discussion](#)

**Bromocarbons in the  
tropical marine  
boundary layer**

L. M. O'Brien et al.

[Title Page](#)[Abstract](#)[Introduction](#)[Conclusions](#)[References](#)[Tables](#)[Figures](#)[⏪](#)[⏩](#)[◀](#)[▶](#)[Back](#)[Close](#)[Full Screen / Esc](#)[Printer-friendly Version](#)[Interactive Discussion](#)

than the averaged flux ( $0.03 \times 10^{-12} \text{ kg m}^{-2} \text{ s}^{-1}$ ) calculated under a mean wind speed of  $6 \text{ ms}^{-1}$  for this period. The high wind speed of  $13 \text{ ms}^{-1}$  clearly exceeds the average wind speed in the tropics, suggesting that sea salt from the open ocean is not the major bromine source maintaining such high BrO concentrations (or that currently accepted air sea flux treatments for aerosol are considerably in error, or that the observationally-based sea salt bromine depletion factor currently used (Yang et al., 2008a) is too low in this region). Alternatively, note that the high BrO is measured at a coastal site, where surf could lead to a significant sea salt production rate even under low wind speeds (de Leeuw et al., 2000). The surf zone could possibly be a potentially large bromine source, although this may be limited to only a relatively narrow region along coasts. Measurements of BrO in the marine boundary layer away from coastal sites would be required to test this possibility. However, if production of BrO is confined to the surf zone, it might be difficult to explain the ozone loss reported by Read et al. (2008).

Figure 7 shows the observed (6 h mean) and simulated ozone during the period 4–12 June (all results are differences, relative to the values at UT=06:00 on 4 June). Throughout the period from 4 to 10 June 2007, the observed ozone declines, with a maximum reduction of more than 20 ppb around 10 June 2007, which corresponds to the period with the very stable boundary layer. The model run without bromine chemistry also shows a similar decline, but with only half the depth of observed peak ozone reduction ( $\sim 10$  ppb). The HiBr run is rather similar to the run without bromine chemistry and again fails to reproduce the magnitude of the observed changes. The model calculation with the increased inorganic bromine source (HiSALT), which leads to BrO levels of around 3 ppt, is closer to the observations and ozone loss is increased up to 4 ppb during this period. The magnitude of the short-fall is largest when the boundary layer is most stable and might be related, for example, to reduced vertical mixing (corresponding to higher BrO concentrations, see Fig. 6, and less entrainment of ozone-rich air from aloft). However, even with elevated BrO of around 3 ppt, this still leaves an ozone decline of more than 5 ppb to be explained by other processes. Given the sporadic high methyl iodide concentrations we have measured, and the high

**Bromocarbons in the  
tropical marine  
boundary layer**

L. M. O'Brien et al.

IO reported by Read et al. (2008), it seems likely that iodine (and iodine-bromine) chemistry is the explanation. This would also be consistent with recent studies in the polar regions (Saiz-Lopez et al., 2007). Note that our 3-D modelled bromine-induced ozone loss is much higher than from the box model calculation by Read et al. (2008).

5 We believe our modelled Br atom concentration must be higher than in their calculation. A major reason could be that our model contains inorganic bromine emissions from sea salt in the form of  $\text{Br}_2$ , which produce Br atoms in sunlight, causing direct ozone loss as a result. Additionally, heterogeneous reactivation on aerosols, as described by Yang et al. (2008b), converts inactive species, such as HBr, to  $\text{Br}_2$ . It seems that  
10 using the observed BrO to constrain the box model (Read et al., 2008) omits these  $\text{Br}_2$  contributions to the Br atom production, especially in marine surface layers where the sea salt source is large. Hence the ozone reduction is smaller.

### 4.3 Use of correlations

Bromocarbon measurements at the coast often show significant correlations, consistent with a common oceanic source. Yokouchi et al. (2005) (see also Carpenter et al., 2003) have exploited the correlations to explore the possible source strengths of the individual species, following McKeen and Liu (1993). For example, a plot of  $\text{CH}_2\text{Br}_2/\text{CHBr}_3$  versus  $\text{CHBr}_3$  often shows a straight line behaviour with the ratio  $\text{CH}_2\text{Br}_2/\text{CHBr}_3$  increasing with decreasing  $\text{CHBr}_3$ . Bromoform ( $\text{CHBr}_3$ ) is the shorter-lived of the two species, so an increase in the ratio would be consistent with more aged air masses, in which  $\text{CHBr}_3$  has been preferentially removed. Alternatively, the plot is also consistent with dilution of the original air mass into a background with higher  $\text{CH}_2\text{Br}_2$  (a likely situation since  $\text{CH}_2\text{Br}_2$  is longer lived). In either case, the smallest ratio of  $\text{CH}_2\text{Br}_2/\text{CHBr}_3$  measured is most consistent with some constant initial emission ratio, since neither mixing nor chemistry can reduce the ratio further.  
25 Assuming that the emissions have common sources and are constant on a regional scale, Yokouchi et al. (2005) use this minimum ratio to define the ratio of the emission sources. When more bromocarbons are measured, a plot of  $\text{CHBr}_3/\text{CH}_2\text{Br}_2$  versus,

[Title Page](#)[Abstract](#)[Introduction](#)[Conclusions](#)[References](#)[Tables](#)[Figures](#)[◀](#)[▶](#)[◀](#)[▶](#)[Back](#)[Close](#)[Full Screen / Esc](#)[Printer-friendly Version](#)[Interactive Discussion](#)

**Bromocarbons in the tropical marine boundary layer**

L. M. O'Brien et al.

[Title Page](#)[Abstract](#)[Introduction](#)[Conclusions](#)[References](#)[Tables](#)[Figures](#)[⏪](#)[⏩](#)[◀](#)[▶](#)[Back](#)[Close](#)[Full Screen / Esc](#)[Printer-friendly Version](#)[Interactive Discussion](#)

say,  $\text{CHBr}_2\text{Cl}/\text{CH}_2\text{Br}_2$ , where  $\text{CH}_2\text{Br}_2$  has the longest lifetime, can also be used, following McKeen and Liu (1993), to derive emission ratios. In this case the data form a triangle, two of whose sides are defined by a “dilution line” (the 1:1 slope for mixing into a zero background) and a “chemical decay line”, defined by the lifetimes of the species.

5 The sides should intersect at a point, which defines the emission ratios.

Figure 8 shows plots of  $\text{CH}_2\text{Br}_2/\text{CHBr}_3$  versus  $\text{CHBr}_3$  for each individual day from 30 May until 15 June 2007 and for all days combined. There is a good correlation throughout the measurement period. The slope for all data is  $-0.74$  with relatively little daily variation throughout the period (a minimum slope of  $-0.51$  on 7 June 2007 and a maximum of  $-0.96$  on 14 June 2007). The data reported in Yokouchi et al. (2005), from the Western Pacific and Christmas Island have a corresponding slope of about  $-0.76$ . The minimum ratio of  $\text{CH}_2\text{Br}_2/\text{CHBr}_3$  does vary a little from day to day but is around 0.06 (with values ranging from 0.06 on 7 June 2007 to 0.19 on 30 May 2007), close to the value given by Yokouchi et al. (2005). 15 June 2007 was the final day of measurements, on which the largest concentrations of several species were measured. The correlation plot for this date is unusual, seeming to consist of two separate populations of points.

Bearing in mind the caveats concerning  $\text{CHBr}_2\text{Cl}$  (discussed in Sect. 2.2), in Fig. 9 we plot  $\text{CHBr}_3/\text{CH}_2\text{Br}_2$  versus  $\text{CHBr}_2\text{Cl}/\text{CH}_2\text{Br}_2$ . The data fit as expected into a region between the 1:1 dilution line and the chemical loss line. They are rather closer to the dilution line, suggesting that the observations might be close to the source region, as also indicated by the diurnal variations evident in  $\text{CHBr}_3$  (see above).

Following Yokouchi et al. (2005) we identify a point, at the top right hand of the figure, with maximum ratios of  $\text{CHBr}_3:\text{CH}_2\text{Br}_2$  and  $\text{CHBr}_2\text{Cl}:\text{CH}_2\text{Br}_2$ . These values vary from day to day; rather than using the absolute maxima we have calculated the values based on 95th percentiles. Given this (perhaps somewhat arbitrary) approach, Fig. 9 indicates an emission ratio for  $\text{CHBr}_3/\text{CH}_2\text{Br}_2$  of about 9 and a value around 0.46 for  $\text{CHBr}_2\text{Cl}/\text{CH}_2\text{Br}_2$ . The former is the same as derived by Yokouchi et al. (2005); the latter is a little smaller, but given the difficulty of our  $\text{CHBr}_2\text{Cl}$  measurement, is in

**Bromocarbons in the  
tropical marine  
boundary layer**

L. M. O'Brien et al.

[Title Page](#)[Abstract](#)[Introduction](#)[Conclusions](#)[References](#)[Tables](#)[Figures](#)[◀](#)[▶](#)[◀](#)[▶](#)[Back](#)[Close](#)[Full Screen / Esc](#)[Printer-friendly Version](#)[Interactive Discussion](#)

good agreement. Note that if we take a different value for  $\text{CHBr}_2\text{Cl}$  in the calibration sample (see Sect. 2.2) the shape of the plot remains the same but is simply shifted horizontally. If we assume a global emission (taken from WMO, 2003) of  $61 \text{ Gg Br yr}^{-1}$  for  $\text{CH}_2\text{Br}_2$ , this leads to global emissions of  $820 \text{ Gg Br yr}^{-1}$  for  $\text{CHBr}_3$  and  $28 \text{ Gg Br yr}^{-1}$  for  $\text{CHBr}_2\text{Cl}$ . Using the higher  $\text{CH}_2\text{Br}_2$  global emission of  $104 \text{ Gg Br yr}^{-1}$  from Warwick et al. (2006), this corresponds to global emissions of  $1404 \text{ Gg Br yr}^{-1}$  for  $\text{CHBr}_3$  and  $48 \text{ Gg Br yr}^{-1}$  for  $\text{CHBr}_2\text{Cl}$ . In either case, these are much higher than estimated in WHO (2003).

Figure 10 plots  $\text{CH}_2\text{Br}_2/\text{CH}_3\text{I}$  versus  $\text{CH}_3\text{I}$ . Like the bromocarbons just considered,  $\text{CH}_3\text{I}$  is expected to have a marine source, but different from the bromocarbons. We see three different periods. From 30 May 2007 to approximately 5 June 2007, and from 10–15 June 2007, there is a good correlation with slope of about  $-0.6$ . This could indicate that the air sampled during these few days has traversed similar source regions, as found above. In contrast between 6 and 8 June 2007, which includes the periods with higher anthropogenic concentrations (see Fig. 3), the correlation is poor and  $\text{CH}_3\text{I}$  concentrations are low at  $\sim 1$  ppt. It seems likely that there has been little recent emission of  $\text{CH}_3\text{I}$  into these air masses.

## 5 Discussion

The  $\mu$ -Dirac gas chromatograph was deployed for several weeks at the Cape Verde observatory. It measured concentrations of a range of anthropogenic and biogenic halocarbons and demonstrated its potential for longterm autonomous measurement. Bromoform ( $\text{CHBr}_3$ ) exhibits the most variability of all the halocarbons observed, ranging from a background concentration of about 3–5 ppt to a maximum of  $>40$  ppt during the course of the measurement period. This range of mixing ratios, and variability, is consistent with previous tropical measurements, particularly those in coastal regions (e.g. Quack et al., 2004; Yokouchi et al., 2005; Carpenter et al., 2007). Dibromomethane ( $\text{CH}_2\text{Br}_2$ ) correlates well with  $\text{CHBr}_3$ , with a slope similar to that reported by Yokouchi

et al. (2005), suggesting a common regional source. Methyl iodide ( $\text{CH}_3\text{I}$ ) does not correlate with these bromocarbons. Base levels of around 1–2 ppt were measured but with some periods of much higher mixing ratios. The indications are that the sources of the biogenic bromocarbons are different to those of  $\text{CH}_3\text{I}$ , as expected.

5 Measurements of  $\text{C}_2\text{Cl}_4$  and  $\text{CHCl}_3$  correlate well with CO and are good indicators of anthropogenic emissions, complementing the biogenic species mentioned above.

In this study, the method following Yokouchi et al. (2005) and McKeen and Liu (1993) is used to derive emission flux ratios for  $\text{CHBr}_3$ ,  $\text{CH}_2\text{Br}_2$  and  $\text{CHBr}_2\text{Cl}$  in the region surrounding Cape Verde. The calculated ratios in this study (9 for  $\text{CHBr}_3:\text{CH}_2\text{Br}_2$  and 0.46 for  $\text{CHBr}_2\text{Cl}:\text{CH}_2\text{Br}_2$ ) are similar to those obtained in the tropics by Yokouchi et al. (2005), but are significantly higher than emission ratios calculated in global studies. For example, the WMO (2003) sink-based bromocarbon emission estimates give molar ratios of 2.3 for  $\text{CHBr}_3:\text{CH}_2\text{Br}_2$  and 0.2 for  $\text{CHBr}_2\text{Cl}:\text{CH}_2\text{Br}_2$ . The Warwick et al. (2006) model study, using a predominantly tropical emission dataset and higher emissions than WMO (2003), gives similar low molar emission ratios of 3.6 for  $\text{CHBr}_3:\text{CH}_2\text{Br}_2$  and 0.2 for  $\text{CHBr}_2\text{Cl}:\text{CH}_2\text{Br}_2$ . A bottom-up study by Butler et al. (2007), which estimated global emissions of  $\text{CHBr}_3$  and  $\text{CH}_2\text{Br}_2$ , based on ship-based observations of surface water and atmospheric concentrations, gives a global emission ratio of 1.9 for  $\text{CHBr}_3:\text{CH}_2\text{Br}_2$ . The large difference between the regional estimates of emission ratios and those obtained from global studies suggests that while regional emission ratios may be valid for near-shore regions, there remains some question over whether (and how) they can be extrapolated on a global scale. Conversely, the strong local emissions may not be included in the global estimates.

25 The global estimates of  $\text{CHBr}_3$  and  $\text{CHBr}_2\text{Cl}$  emissions derived in this study depend not only upon uncertainty in the global extrapolation, but also the value chosen for  $\text{CH}_2\text{Br}_2$  emissions. Although  $\text{CH}_2\text{Br}_2$  emissions are believed to be better constrained than other bromocarbons due to its longer lifetime, there is still significant uncertainty in global emission estimates. The WMO (2003) sink-based estimate ( $66 \text{ Gg CH}_2\text{Br}_2 \text{ yr}^{-1}$ ) is significantly smaller than the emissions required by the 3-D model study by Warwick

---

**Bromocarbons in the tropical marine boundary layer**L. M. O'Brien et al.

---

[Title Page](#)[Abstract](#)[Introduction](#)[Conclusions](#)[References](#)[Tables](#)[Figures](#)[◀](#)[▶](#)[◀](#)[▶](#)[Back](#)[Close](#)[Full Screen / Esc](#)[Printer-friendly Version](#)[Interactive Discussion](#)

et al. (2006) to reproduce observations based on a predominantly tropical emission dataset ( $113 \text{ Gg CH}_2\text{Br}_2 \text{ yr}^{-1}$ ). This demonstrates that even for  $\text{CH}_2\text{Br}_2$ , the geographical distribution of its emissions can have an important impact on the global atmospheric lifetime and thus the global sink-based emission estimate. To resolve the emissions clearly calls for a measurement/modelling programme involving both local and global measurements.

Even when the local emissions in the model are increased to allow a reasonable representation of the observed bromocarbons at Cape Verde, the modelled BrO is well below the observed 2–3 ppt reported by Read et al. (2008). Very short-lived bromocarbons might explain part of this shortfall but it seems more likely that the source could be inorganic, from sea salt emissions. These had to be increased very substantially to match the high BrO, implying unrealistically high regional wind speeds across the ocean surface. Alternatively, it could be that the parameterisation of sea-salt aerosol production over the open ocean is inadequate. Despite the low winds in the region, we noted the ubiquitous presence of sea salt deposits on buildings, etc. It seems possible that a very local source, associated with the coastal surf zone, could be playing a role. Measurements of BrO in the free marine boundary layer could help to resolve this question.

Throughout the period of our halocarbon measurements, and especially from 4 to 10 June, the observed ozone declines, with a maximum reduction of about 20 ppb around 10 June, which corresponds to the period with a very stable boundary layer. When high BrO is modelled by artificially increasing the sea salt source we do reproduce part of the observed ozone decline (perhaps by 3–4 ppb, still leaving about 5 ppb ozone decline to be explained by other processes). The magnitude of the short-fall is largest when the boundary layer is most stable and might be related to increased deposition. However, this is a slow process in the marine boundary layer and other chemical explanations seem more likely. For example, if a very local source of the halogens is operating, its effect would be most evident under these stable conditions. However, given the sporadic high concentrations of methyl iodide we have measured, and the

## Bromocarbons in the tropical marine boundary layer

L. M. O'Brien et al.

Title Page

Abstract

Introduction

Conclusions

References

Tables

Figures

◀

▶

◀

▶

Back

Close

Full Screen / Esc

Printer-friendly Version

Interactive Discussion



high IO reported by Read et al. (2008), it seems likely that iodine (and iodine-bromine) chemistry is an important part of the explanation.

*Acknowledgements.* This work was supported by NERC, NCAS and by the European Commission through the SCOUT-O3 project (505390-GOCE-CF2004). Louise O'Brien thanks NERC for a research studentship. Andrew Robinson acknowledges NERC for their support through small grant project NE/D008085/1. We thank James Lee, Katie Read, Alastair Lewis and Lucy Carpenter from the University of York, UK, and Luis Mendes and Paulo Mendes from INMG, Cape Verde, for allowing us to use their CO and O<sub>3</sub> data in this paper. We acknowledge the British Atmospheric Data Centre (BADC) web trajectory service, and also thank Dickon Young and Simon O'Doherty at the University of Bristol for useful correspondence.

## References

- Barrie, L. A., Bottenheim, J. W., Schnell, R. C., Crutzen, P. J., and Rasmussen, R. A.: Ozone destruction and photochemical reactions at polar sunrise in the lower Arctic atmosphere, *Nature*, 334, 138–141, 1988.
- Bassford, M. R., Nickless, G., Simmonds, P. G., Lewis, A. C., Pilling, M. J., and Evans, M. J.: The concurrent observation of methyl iodide and dimethyl sulphide in marine air: implications for sources of atmospheric methyl iodide, *Atmos. Environ.*, 33, 2373–2383, 1999.
- Butler, J. H., King, D. B., Lobert, J. M., Montzka, S. A., Yvon-Lewis, S. A., Hall, B. D., Warwick, N. J., Mondeel, D. J., Aydin, M., and Elkins, J. W.: Oceanic distributions and emissions of short-lived halocarbons, *Global Biogeochem. Cy.*, 21, GB1023, doi:10.1029/2006GB002732, 2007.
- Carpenter, L. J. and Liss, P. S.: On temperate sources of bromoform and other reactive bromine gases, *J. Geophys. Res.*, 105(D12), 20539–20547, 2000.
- Carpenter, L. J., Liss, P. S., and Penkett, S. A.: Marine organohalogens in the atmosphere over the Atlantic and Southern Oceans, *J. Geophys. Res.*, 108(D9), 4256, doi:10.1029/2002JD002769, 2003.
- Carpenter, L. J., Wevill, D. J., O'Doherty, S., Spain, G., and Simmonds, P. G.: Atmospheric bromoform at Mace Head, Ireland: seasonality and evidence for a peatland source, *Atmos. Chem. Phys.*, 5, 2927–2934, 2005, <http://www.atmos-chem-phys.net/5/2927/2005/>.

## Bromocarbons in the tropical marine boundary layer

L. M. O'Brien et al.

Title Page

Abstract

Introduction

Conclusions

References

Tables

Figures

◀

▶

◀

▶

Back

Close

Full Screen / Esc

Printer-friendly Version

Interactive Discussion



**Bromocarbons in the  
tropical marine  
boundary layer**

L. M. O'Brien et al.

Title Page

Abstract

Introduction

Conclusions

References

Tables

Figures

◀

▶

◀

▶

Back

Close

Full Screen / Esc

Printer-friendly Version

Interactive Discussion

Carpenter, L., Wevill, D. J., Hopkins, J. R., Dunk, R. M., Jones, C. E., Hornsby, K. E., and McQuaid, J. B.: Bromoform in tropical Atlantic air from 25° N to 25° S, *Geophys. Res. Lett.*, 34, L11810, doi:10.1029/2007/GL029893, 2007.

Carpenter, L. J., Jones, C. E., Dunk, R. M., and Hornsby, K. E.: Air-sea fluxes of biogenic bromine from the tropical and North Atlantic Ocean, *Atmos. Chem. Phys. Discuss.*, 8, 18409–18435, 2008,  
http://www.atmos-chem-phys-discuss.net/8/18409/2008/.

Chipperfield, M. P. and Pyle, J. A.: Model sensitivity studies of Arctic ozone depletion, *J. Geophys. Res.*, 103(D19), 28398–28403, 1998.

Class, T. H. and Ballschmiter, K.: Chemistry of organic traces in air: sources and distribution of bromo- and bromochloromethanes in marine air and surfacewater of the Atlantic Ocean, *J. Atmos. Chem.*, 6, 35–46, 1988.

Cook, P. A., Savage, N. H., Turquety, S., Carver, G. D., O'Connor, F. M., Heckel, A., Stewart, D., Whalley, L. K., Parker, A. E., Schlager, H., Singh, H. B., Avery, M. A., Sachse, G. W., Brune, W., Richter, A., Burrows, J. P., Purvis, R., Lewis, A. C., Reeves, C. E., Monks, P. S., Levine, J. G., and Pyle, J. A.: Forest fire plumes over the North Atlantic: p-TOMCAT model simulations with aircraft and satellite measurements from the ITOP/ICARTT campaign, *J. Geophys. Res.*, 112, D10S43, doi:10.1029/2006JD007563, 2007.

de Leeuw, G., Neele, F., Hill, M., Smith, M., and Vignati, E.: Production of sea spray aerosol in the surf zone, *J. Geophys. Res.*, 105(D24), 29397–29409, 2000.

Dessler, M.: Selective gas chromatographic detectors, *J. Chromatog. Libr.*, 36, 1986.

Ekdahl, A., Pedersén, M., and Abrahamsson, K.: A study of the diurnal variation of biogenic volatile halocarbons, *Mar. Chem.*, 63, 1–8, 1998.

Goodwin, K. D., North, W. J., and Lidstrom, M. E.: Production of bromoform and dibromomethane by giant kelp: Factors affecting release and comparison to anthropogenic bromine sources, *Limnol. Oceanogr.*, 42, 8, 1725–1734, 1997.

Gostlow, B., Robinson, A. D., Pyle, J. A., Harris, N. R. P., and O'Brien, L. M.:  $\mu$ -Dirac: An autonomous instrument for halocarbon measurements, in preparation, 2009.

Grose, M. R., Caine, J. M., McMinn, A., and Gibson, J. A. E.: Coastal marine methyl iodide source and links to new particle formation at Cape Grim during February 2006, *Environ. Chem.*, 4, 172–177, 2007.

Hoekstra, E. J., De Leer, E. W. B., and Brinkman, U. A. T.: Natural Formation of Chloroform and Brominated Trihalomethanes in Soil, *Environ. Sci. Technol.*, 32, 3724–3729, 1998.



**Bromocarbons in the  
tropical marine  
boundary layer**

L. M. O'Brien et al.

[Title Page](#)[Abstract](#)[Introduction](#)[Conclusions](#)[References](#)[Tables](#)[Figures](#)[◀](#)[▶](#)[◀](#)[▶](#)[Back](#)[Close](#)[Full Screen / Esc](#)[Printer-friendly Version](#)[Interactive Discussion](#)

Khalil, M. A. K., Moore, R., Harper, D., Lobert, J., Erickson, D., Koropalov, V., Sturges, W., and Keene, W.: Natural emissions of chlorine-containing gases: Reactive chlorine emissions inventory, *J. Geophys. Res.* 104(D7), 8333–8346, 1999.

Law, K., Plantevin, P.-H., Thouret, V., Marengo, A., Asman, W., Lawrence, M., Crutzen, P., Muller, J. F., Hauglustaine, D., and Kanakidou, M.: Comparison between global chemistry transport model results and measurement of Ozone and Water Vapour by Airbus-In-Service Aircraft (MOZAIC) data, *J. Geophys. Res.*, 105(D1), 1503–1525, 2000.

Lovelock, J. E.: Ionization methods for the analysis of gases and vapours, *Anal. Chem.*, 33(2), 162–178, 1961.

McKeen, S. A. and Liu, S. C.: Hydrocarbon ratios and photochemical history of air masses, *Geophys. Res. Lett.*, 20, 2363–2366, 1993.

Monahan, E. C., Spiel, D. E., and Davidson, K. L.: A model of marine aerosol generation via whitecaps and wave disruption, in: *Oceanic Whitecaps*, edited by: Monahan, E. C. and Mac Niocail, G., Reidel, D., and Norwell, M. A., 167–174, 1986.

Moore, R. M. and Tokarczyk, R.: Volatile biogenic halocarbons in the northwest Atlantic, *Global Biogeochem. Cy.*, 7, 195–210, 1993.

Norton, T. A. and Mathieson, A. C.: The biology of unattached seaweeds, in: *Progress in Physiological Research*, edited by: Round, F. and Chapman, D., Elsevier Sci. Publ., Amsterdam, 2, 333–386, 1983.

Pellizzari, E. D.: Electron Capture Detection in Gas Chromatography, *J. Chromatogr.*, 98, 323–361, 1974.

Penkett, S. A., Jones, B. M. R., and Rycroft, M. J.: An interhemispheric comparison of the concentrations of bromine compounds in the atmosphere, *Nature*, 318, 550–553, 1985.

Pradhan, Y., Lavender, S. J., Hardman-Mountford, N. J., and Aiken, J.: Seasonal and inter-annual variability of chlorophyll-a concentration in the Mauritanian upwelling: Observation of an anomalous event during 1998–1999, *Deep Sea Research II*, 53, 1548–1559, 2006.

Quack, B. and Wallace, D. W. R.: Air-sea flux of bromoform: Controls, rates and implications, *Global. Biogeochem. Cy.*, 17(1), 1023, doi:10.1029/2002GB001890, 2003.

Quack, B., Atlas, E., Petrick, G., Schauffler, S., and Wallace, D.: Oceanic bromoform sources for the tropical atmosphere, *Geophys. Res. Lett.*, 31, L23505, doi:10.1029/2004GL020597, 2004.

Quack, B., Peeken, I., Petrick, G., and Nachtigall, K.: Oceanic distribution and sources of bromoform and dibromomethane in the Mauritanian upwelling, *J. Geophys. Res.*, 112, C100006,

doi:10.1029/2006JC003803, 2007.

- Read, K. A., Mahajan, A. S., Carpenter, L. J., Evans, M. J., Faria, B. V. E., Heard, D. E., Hopkins, J. R., Lee, J. D., Moller, S. J., Lewis, A. C., Mendes, L., McQuaid, J. B., Oetjen, H., Saiz-Lopez, A., Pilling, M. J., and Plane, J. M. C.: Extensive halogen-mediated ozone destruction over the tropical Atlantic Ocean, *Nature*, 453, 1232–1235, doi:10.1038/nature07035, 2008.
- Rivett, A. C., Martin, D., Nickless, G., Simmonds, P. G., O'Doherty, S. J., Gray, D. J., and Shallcross, D. E.: In situ gas chromatographic measurements of halocarbons in an urban environment, *Atmos. Environ.*, 37, 2221–2235, 2003.
- Robinson, A. D., McIntyre, J., Harris, N. R. P., Pyle, J. A., Simmonds, P. G., and Danis, F.: A lightweight balloon-borne gas chromatograph for in-situ measurements of atmospheric halocarbons, *Rev. Sci. Instrum.*, 71, 4553–4560, 2000.
- Robinson, A. D., Millard, G. A., Danis, F., Guirlet, M., Harris, N. R. P., Lee, A. M., McIntyre, J. D., Pyle, J. A., Arvelius, J., Dagnesjo, S., Kirkwood, S., Nilsson, H., Toohey, D. W., Deshler, T., Goutail, F., Pommereau, J.-P., Elkins, J. W., Moore, F., Ray, E., Schmidt, U., Engel, A., and Mller, M.: Ozone loss derived from balloon-borne tracer measurements in the 1999/2000 Arctic winter, *Atmos. Chem. Phys.*, 5, 1423–1436, 2005, <http://www.atmos-chem-phys.net/5/1423/2005/>.
- Ross, D. E. M., Pyle, J. A., Harris, N. R. P., McIntyre, J. D., Millard, G. A., Robinson A. D. and Busen R.: Investigation of Arctic O<sub>3</sub> depletion sampled over midlatitudes during the Egrett campaign of spring/summer 2000, *Atmos. Chem. Phys.*, 4, 1407–17, 2004, <http://www.atmos-chem-phys.net/4/1407/2004/>.
- Saiz-Lopez, A., Mahajan, A. S., Salmon, R. A., Bauguitte, S. J.-B, Jones, A. E., Roscoe, H. K., and Plane, J. M. C.: Boundary Layer Halogens in Coastal Antarctica, *Science*, 317, 348–351, 2007.
- Salawitch, R. J.: Biogenic bromine, *Nature*, 439, 275–277, 2006.
- Savage, N. H., Law, K. S., Pyle, J. A., Richter, A., Nüß, H., and Burrows, J. P.: Using GOME NO<sub>2</sub> satellite data to examine regional differences in TOMCAT model performance, *Atmos. Chem. Phys.*, 4, 1895–1912, 2004, <http://www.atmos-chem-phys.net/4/1895/2004/>.
- Schall, C., Heumann, K. G., and Kirst, G. O.: Biogenic volatile organoiodine and organobromine hydrocarbons in the Atlantic Ocean from 42° N to 72° S, *Fresen. J. Anal. Chem.*, 359, 298–305, 1997.
- Thomas, A. C., Carr, M.-E., and Strub, P. T.: Chlorophyll variability in eastern boundary currents,

**Bromocarbons in the tropical marine boundary layer**

L. M. O'Brien et al.

Title Page

Abstract

Introduction

Conclusions

References

Tables

Figures

◀

▶

◀

▶

Back

Close

Full Screen / Esc

Printer-friendly Version

Interactive Discussion



- Geophys. Res. Lett., 28, 18, 3421–3424, 2001.
- von Glasow, R., von Kuhlmann, R., Lawrence, M. G., Platt, U., and Crutzen, P. J.: Impact of reactive bromine chemistry in the troposphere, *Atmos. Chem. Phys.*, 4, 2481–2497, 2004, <http://www.atmos-chem-phys.net/4/2481/2004/>.
- 5 Warwick, N. J., Pyle, J. A., Carver, G. D., Yang, X., Savage, N. H., O'Connor, F. M., and Cox, R. A.: Global modeling of biogenic bromocarbons, *J. Geophys. Res.*, 111, D24305, doi:10.1029/2006JD007264, 2006.
- World Meteorological Organisation (WMO): Scientific Assessment of Ozone Depletion: Global ozone research and monitoring project, Rep. 47., World Meteorol. Org., Geneva, 2003.
- 10 World Meteorological Organisation (WMO): Scientific Assessment of Ozone Depletion 2006: Global ozone research and monitoring project, Rep. 50., World Meteorol. Org., Geneva, 2007.
- Yang, X., Cox, R. A., Warwick, N. J., Pyle, J. A., Carver, G. D., O'Connor, F. M., and Savage, N. H.: Tropospheric bromine chemistry and its impacts on ozone: A model study, *J. Geophys. Res.*, 110, D23311, doi:10.1029/2005JD006244, 2005.
- 15 Yang, X., Pyle, J. A., and Cox, R. A.: Sea salt aerosol production and bromine release: Role of snow on sea ice, *Geophys. Res. Lett.*, 35, L16815, doi:10.1029/2008GL034536, 2008a.
- Yang, X., Pyle, J. A., and Cox, R. A.: Blowing snow on sea ice, polar explosions and global ozone, in review, 2008b.
- 20 Yokouchi, Y., Hasebe, F., Fujiwara, M., Takashima, H., Shiotani, M., Nishi, N., Kanaya, Y., Hashimoto, S., Fraser, P., Toom-Sauntry, D., Mukai, H., and Nojiri, Y.: Correlations and emission ratios among bromoform, dibromochloromethane, and dibromomethane in the atmosphere, *J. Geophys. Res.*, 110, D23309, doi:10.1029/2005JD006303, 2005.

---

**Bromocarbons in the  
tropical marine  
boundary layer**L. M. O'Brien et al.

---

[Title Page](#)[Abstract](#)[Introduction](#)[Conclusions](#)[References](#)[Tables](#)[Figures](#)[◀](#)[▶](#)[◀](#)[▶](#)[Back](#)[Close](#)[Full Screen / Esc](#)[Printer-friendly Version](#)[Interactive Discussion](#)

## Bromocarbons in the tropical marine boundary layer

L. M. O'Brien et al.

**Table 1.** Measurement characteristics during the Cape Verde deployment of  $\mu$ -Dirac. The precisions are the single standard deviations (in %) of the measurements of the calibration standards. The accuracies for  $\text{CH}_3\text{I}$ ,  $\text{CH}_2\text{Br}_2$ ,  $\text{CHBr}_3$ ,  $\text{C}_2\text{Cl}_4$ , and  $\text{CHCl}_3$  are taken from the values quoted with the NOAA-ESRL supplied standard. The accuracy for  $\text{CHBr}_2\text{Cl}$  is estimated as 50% since no value is available for the amount in the calibration standard (see text). The detection limits are estimated from the signal to noise ratio (average calibration peak height/RMS of the noise level (blank samples)), using the known amount of a compound in the calibration gas to deduce the smallest detectable concentration. See Gostlow et al. (2009) for more details.

Species	$\text{CH}_3\text{I}$	$\text{CH}_2\text{Br}_2$	$\text{CHBr}_3$	$\text{C}_2\text{Cl}_4$	$\text{CHCl}_3$	$\text{CHBr}_2\text{Cl}$
Precision	8.4%	4%	3.2%	1.6%	1.4%	9.6%
Accuracy	3%	2.1%	2.2%	3%	1%	50%
Detection limit	0.3 ppt	0.1 ppt	0.4 ppt	0.2 ppt	0.7 ppt	0.02 ppt

Title Page

Abstract

Introduction

Conclusions

References

Tables

Figures

◀

▶

◀

▶

Back

Close

Full Screen / Esc

Printer-friendly Version

Interactive Discussion



## Bromocarbons in the tropical marine boundary layer

L. M. O'Brien et al.

**Table 2.** Summary of selected halocarbon data ( $\text{CHBr}_3$ ,  $\text{CH}_2\text{Br}_2$ ,  $\text{CH}_3\text{I}$ ,  $\text{CHCl}_3$ ) collected at the Cape Verde Observatory from 30 May to 15 June 2007. The range (minimum to maximum) and mean (with standard deviation in brackets) are given, for each of the four species and for each day of the campaign. The number of samples each day was usually more than 80 (with the exception of 1, 5, 11, 14 and 15 June, which had 55, 65, 65, 41 and 59 samples, respectively).

Date	$\text{CHBr}_3$		$\text{CH}_2\text{Br}_2$		$\text{CH}_3\text{I}$		$\text{CHCl}_3$	
	Range	Mean (S.D.)	Range	Mean (S.D.)	Range	Mean (S.D.)	Range	Mean (S.D.)
30-Jun	2.8–11.5	5.3 (1.6)	1.4–2.6	2.0 (0.2)	1.7–4.9	2.7 (0.7)	15.3–19.3	17.4 (1.0)
31-May	2.8–11.9	5.2 (1.8)	1.0–2.6	1.8 (0.3)	1.0–4.4	2.1 (0.8)	14.3–18.2	16.0 (0.9)
01-Jun	2.4–19.7	5.5 (3.4)	1.1–2.7	1.6 (0.4)	0.9–4.8	1.5 (0.7)	12.8–17.5	14.9 (1.7)
02-Jun	3.3–19.9	6.9 (3.2)	1.1–2.6	1.8 (0.3)	1.0–4.1	2.1 (0.6)	11.8–19.4	14.7 (1.9)
03-Jun	2.5–12.7	6.0 (2.7)	1.0–2.4	1.6 (0.3)	1.2–3.4	1.9 (0.5)	15.1–18.1	16.8 (0.7)
04-Jun	2.0–11.1	4.3 (2.0)	0.9–2.7	1.4 (0.3)	1.2–3.9	1.8 (0.6)	15.1–20.3	17.6 (1.0)
05-Jun	2.3–23.2	6.7 (3.6)	1.0–2.7	1.5 (0.3)	0.7–2.6	1.3 (0.4)	17.4–20.0	18.6 (0.6)
06-Jun	3.3–27.2	9.8 (4.9)	0.9–2.6	1.6 (0.3)	1.0–2.0	1.4 (0.2)	13.8–18.3	16.0 (1.1)
07-Jun	3.2–43.7	13.5 (8.0)	0.7–3.2	1.6 (0.5)	0.9–1.4	1.2 (0.1)	11.6–14.2	13.1 (0.6)
08-Jun	3.5–42.5	12.6 (7.0)	0.8–3.1	1.5 (0.4)	1.0–1.7	1.3 (0.2)	11.7–14.7	13.2 (0.7)
09-Jun	2.8–20.9	7.8 (4.0)	0.9–2.8	1.7 (0.5)	1.2–5.0	1.9 (0.9)	12.2–16.3	14.2 (0.9)
10-Jun	3.5–16.1	6.0 (1.9)	1.5–2.9	2.3 (0.3)	1.5–6.0	3.6 (1.0)	17.1–22.5	19.9 (1.2)
11-Jun	3.0–11.8	5.3 (1.9)	1.6–2.7	2.0 (0.3)	2.0–5.3	3.3 (0.7)	19.1–21.9	20.4 (0.6)
14-Jun	5.7–25.5	11.8 (4.2)	1.8–3.1	2.5 (0.3)	0.9–4.9	3.1 (1.4)	14.3–17.8	15.8 (1.1)
15-Jun	4.9–27.2	13.1 (5.0)	1.7–8.8	4.6 (1.8)	0.5–31.4	13.8 (8.9)	13.7–22.9	19.1 (2.2)

Title Page

Abstract

Introduction

Conclusions

References

Tables

Figures

◀

▶

◀

▶

Back

Close

Full Screen / Esc

Printer-friendly Version

Interactive Discussion



25 May 2007

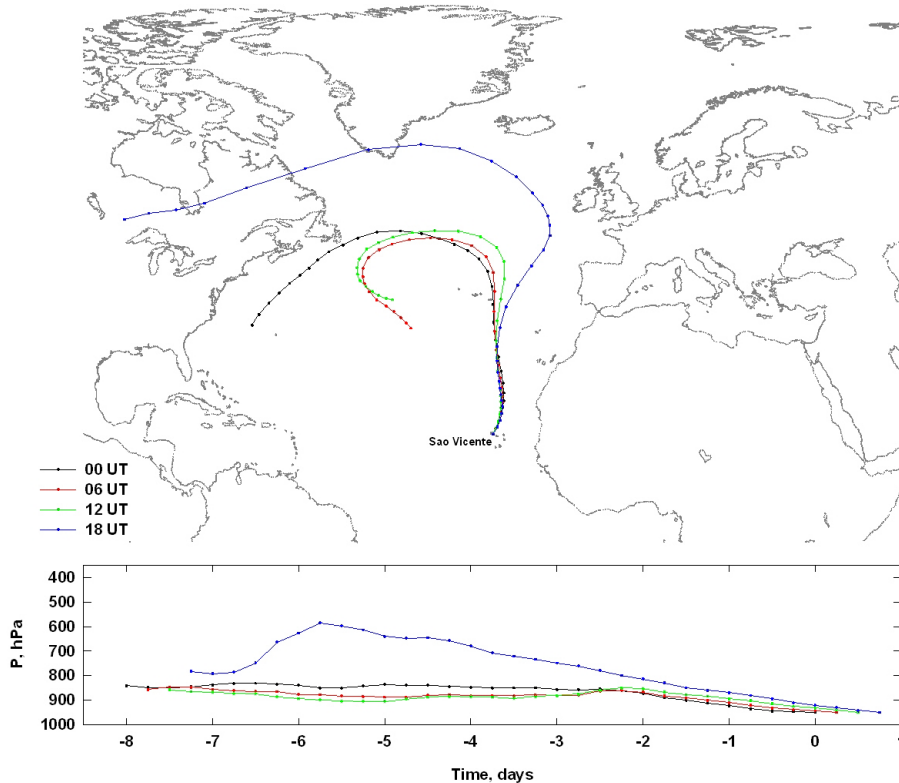


**Fig. 1a.** 8-day back trajectories obtained from the British Atmospheric Data Centre (BADC), shown on a latitude-longitude plot and a pressure-time plot. Trajectories arrive at 950 hPa at the Cape Verde Observatory, Sao Vicente. There are four trajectories per day (at 00:00:00, 06:00:00, 12:00:00 and 18:00:00 UT).

**Bromocarbons in the tropical marine boundary layer**

L. M. O'Brien et al.

Title Page

Abstract

Introduction

Conclusions

References

Tables

Figures

◀

▶

◀

▶

Back

Close

Full Screen / Esc

Printer-friendly Version

Interactive Discussion



**Bromocarbons in the  
tropical marine  
boundary layer**

L. M. O'Brien et al.

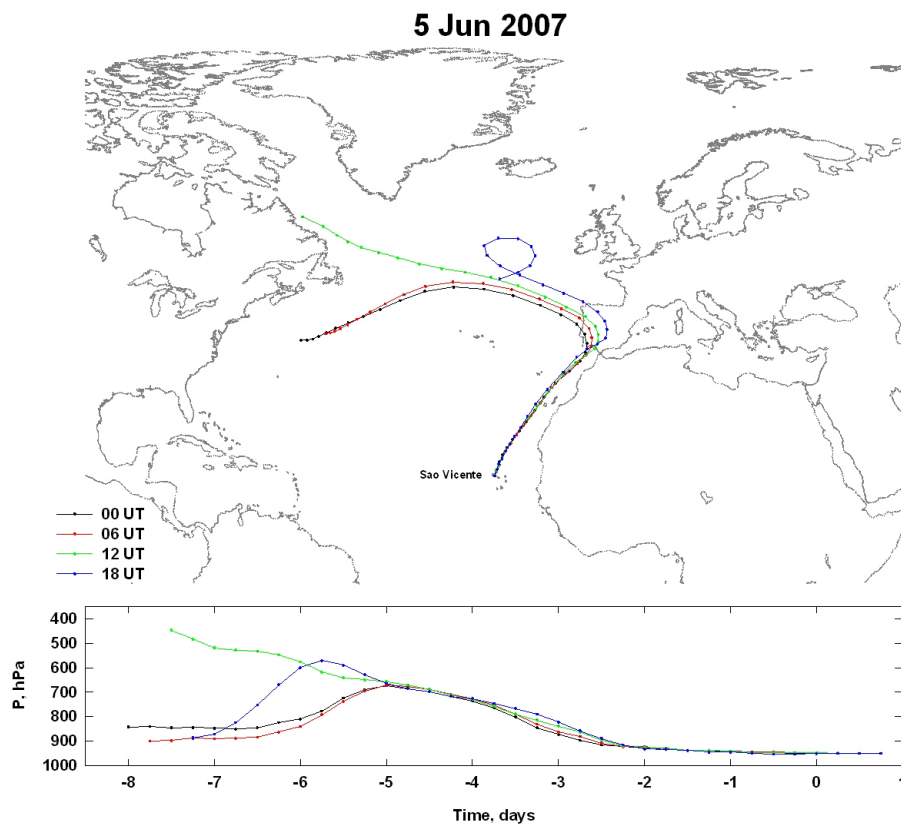
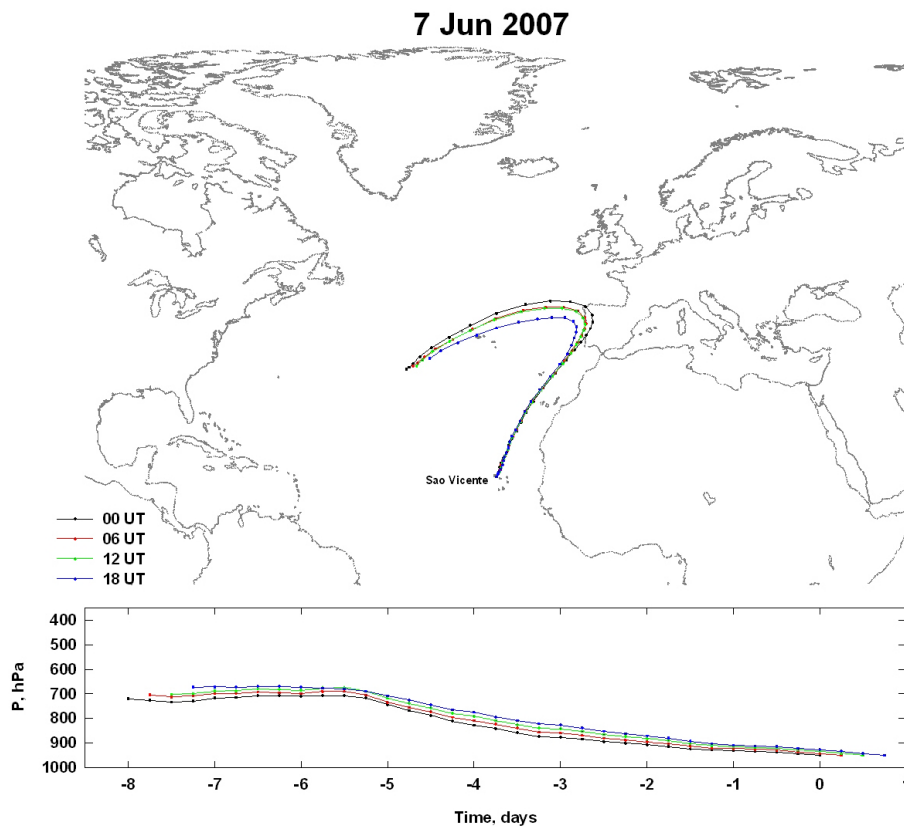


Fig. 1b. Continued.

[Title Page](#)[Abstract](#)[Introduction](#)[Conclusions](#)[References](#)[Tables](#)[Figures](#)[◀](#)[▶](#)[◀](#)[▶](#)[Back](#)[Close](#)[Full Screen / Esc](#)[Printer-friendly Version](#)[Interactive Discussion](#)

**Bromocarbons in the  
tropical marine  
boundary layer**

L. M. O'Brien et al.

**Fig. 1c.** Continued.[Title Page](#)[Abstract](#)[Introduction](#)[Conclusions](#)[References](#)[Tables](#)[Figures](#)[◀](#)[▶](#)[◀](#)[▶](#)[Back](#)[Close](#)[Full Screen / Esc](#)[Printer-friendly Version](#)[Interactive Discussion](#)

**Bromocarbons in the  
tropical marine  
boundary layer**

L. M. O'Brien et al.

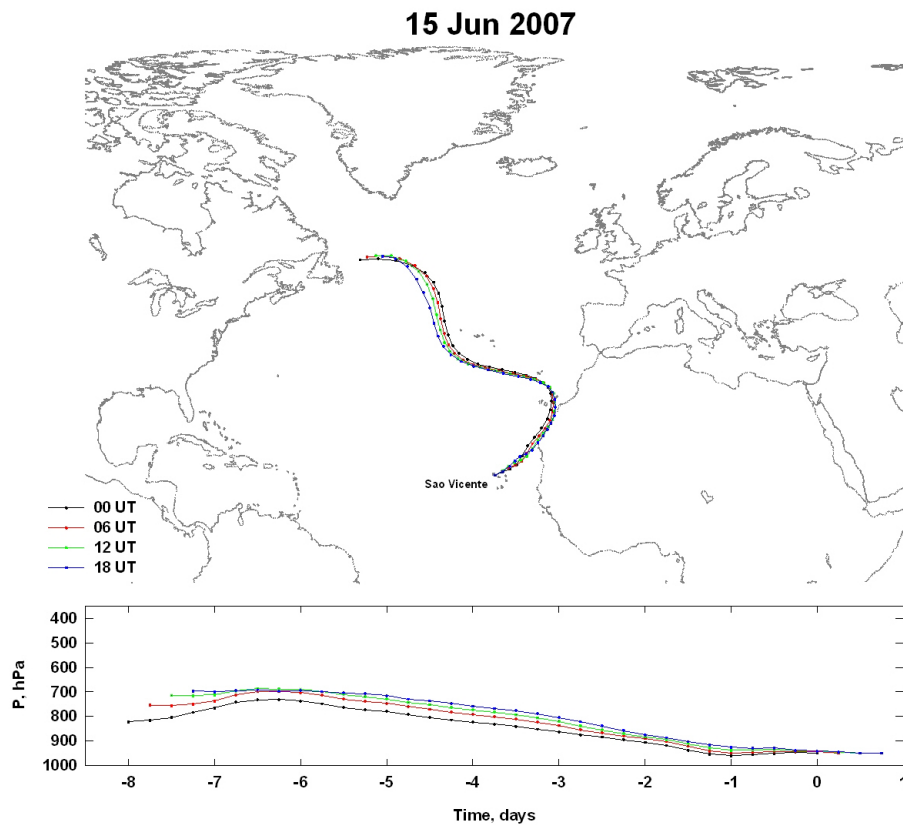
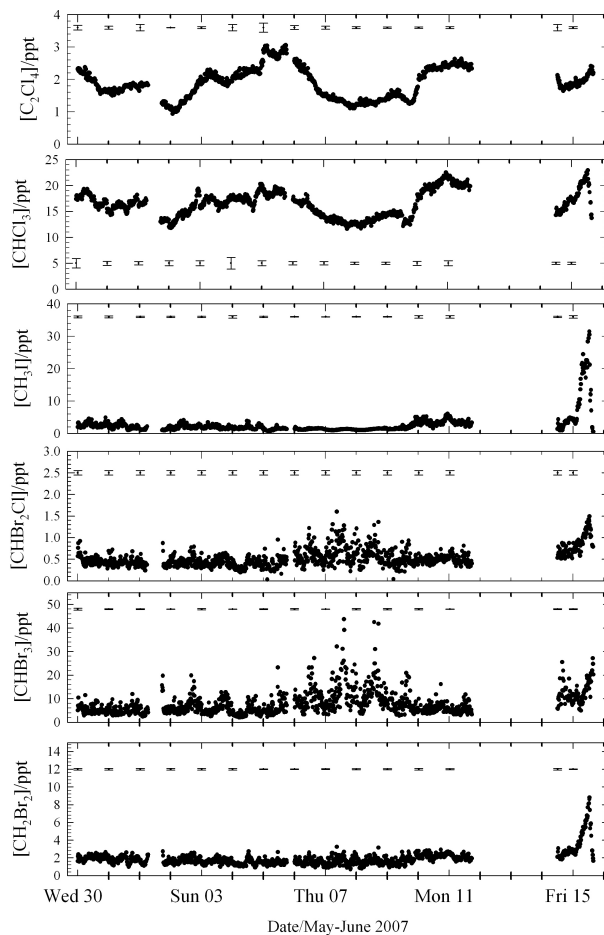


Fig. 1d. Continued.

[Title Page](#)[Abstract](#)[Introduction](#)[Conclusions](#)[References](#)[Tables](#)[Figures](#)[◀](#)[▶](#)[◀](#)[▶](#)[Back](#)[Close](#)[Full Screen / Esc](#)[Printer-friendly Version](#)[Interactive Discussion](#)

**Bromocarbons in the  
tropical marine  
boundary layer**

L. M. O'Brien et al.



**Fig. 2.** Time series plots of  $C_2Cl_4$ ,  $CHCl_3$ ,  $CH_3I$ ,  $CHBr_2Cl$ ,  $CHBr_3$  and  $CH_2Br_2$ . The error bars shown are calculated each day. These are  $\pm 1\sigma$  error bars and are the precision estimates.

[Title Page](#)[Abstract](#)[Introduction](#)[Conclusions](#)[References](#)[Tables](#)[Figures](#)[◀](#)[▶](#)[◀](#)[▶](#)[Back](#)[Close](#)[Full Screen / Esc](#)[Printer-friendly Version](#)[Interactive Discussion](#)

**Bromocarbons in the  
tropical marine  
boundary layer**

L. M. O'Brien et al.

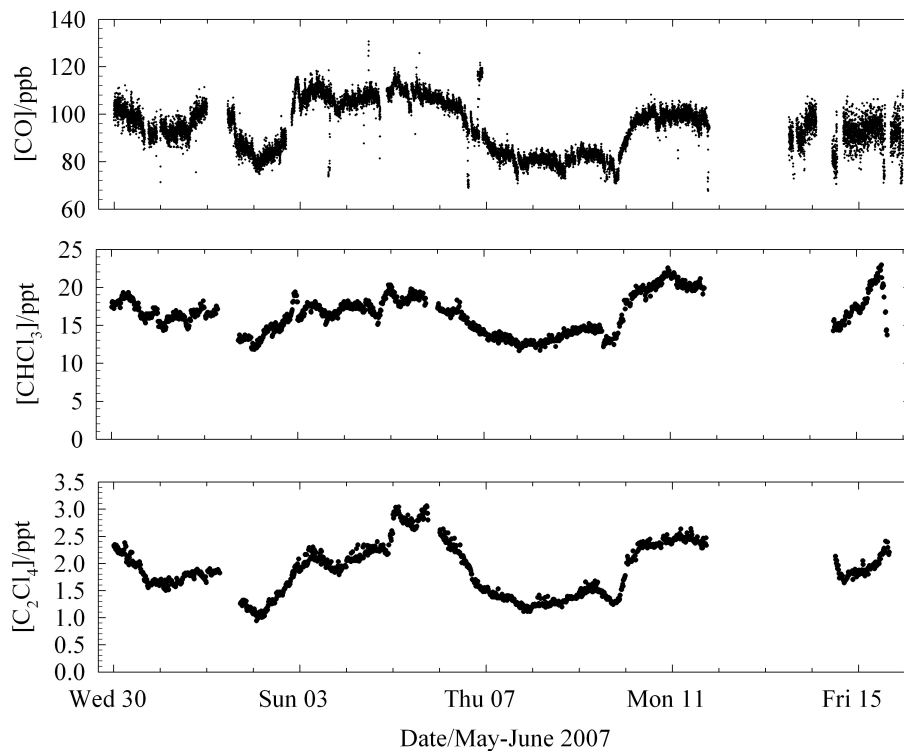


**Fig. 3.** Time series plots of CO (data courtesy of University of York), CHCl<sub>3</sub> and C<sub>2</sub>Cl<sub>4</sub>.

[Title Page](#)[Abstract](#)[Introduction](#)[Conclusions](#)[References](#)[Tables](#)[Figures](#)[◀](#)[▶](#)[◀](#)[▶](#)[Back](#)[Close](#)[Full Screen / Esc](#)[Printer-friendly Version](#)[Interactive Discussion](#)

**Bromocarbons in the  
tropical marine  
boundary layer**

L. M. O'Brien et al.

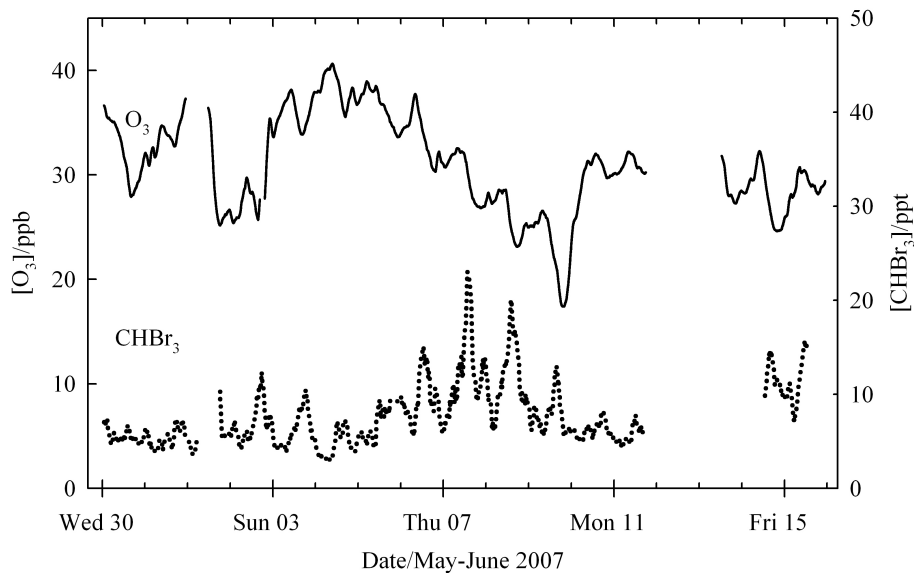


**Fig. 4.** Two-hourly running mean of surface ozone (data courtesy of University of York) and  $CHBr_3$ .

[Title Page](#)[Abstract](#)[Introduction](#)[Conclusions](#)[References](#)[Tables](#)[Figures](#)[◀](#)[▶](#)[◀](#)[▶](#)[Back](#)[Close](#)[Full Screen / Esc](#)[Printer-friendly Version](#)[Interactive Discussion](#)

**Bromocarbons in the  
tropical marine  
boundary layer**

L. M. O'Brien et al.

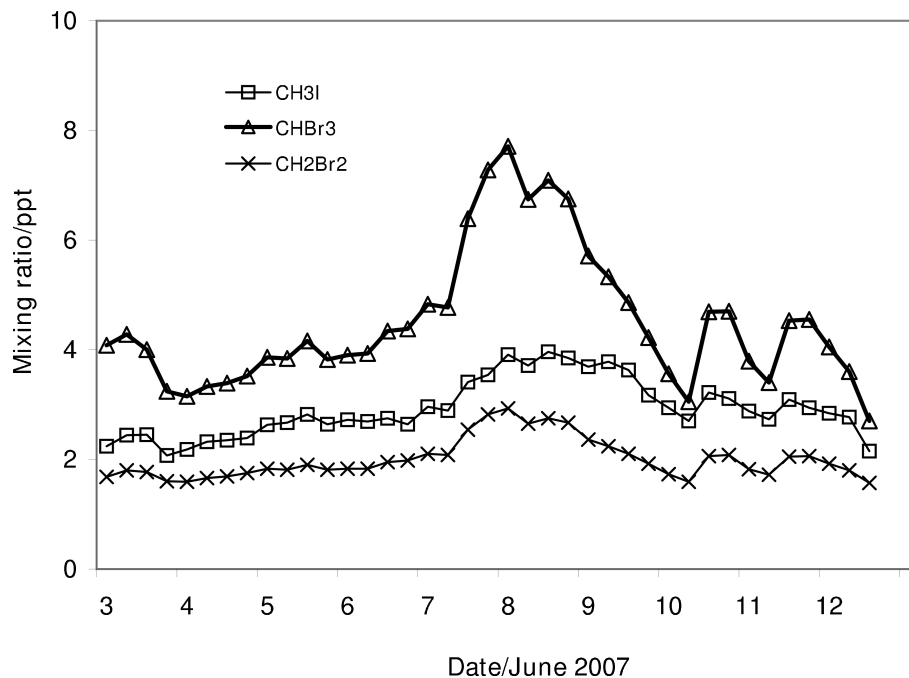


**Fig. 5.** Simulated  $\text{CH}_3\text{I}$ ,  $\text{CH}_2\text{Br}_2$  and  $\text{CHBr}_3$  over Cape Verde after scaling up the emission flux for each species within the region  $10\text{--}20^\circ\text{N}$ ,  $20\text{--}30^\circ\text{W}$  (covering the Cape Verde islands).

[Title Page](#)[Abstract](#)[Introduction](#)[Conclusions](#)[References](#)[Tables](#)[Figures](#)[◀](#)[▶](#)[◀](#)[▶](#)[Back](#)[Close](#)[Full Screen / Esc](#)[Printer-friendly Version](#)[Interactive Discussion](#)

**Bromocarbons in the  
tropical marine  
boundary layer**

L. M. O'Brien et al.

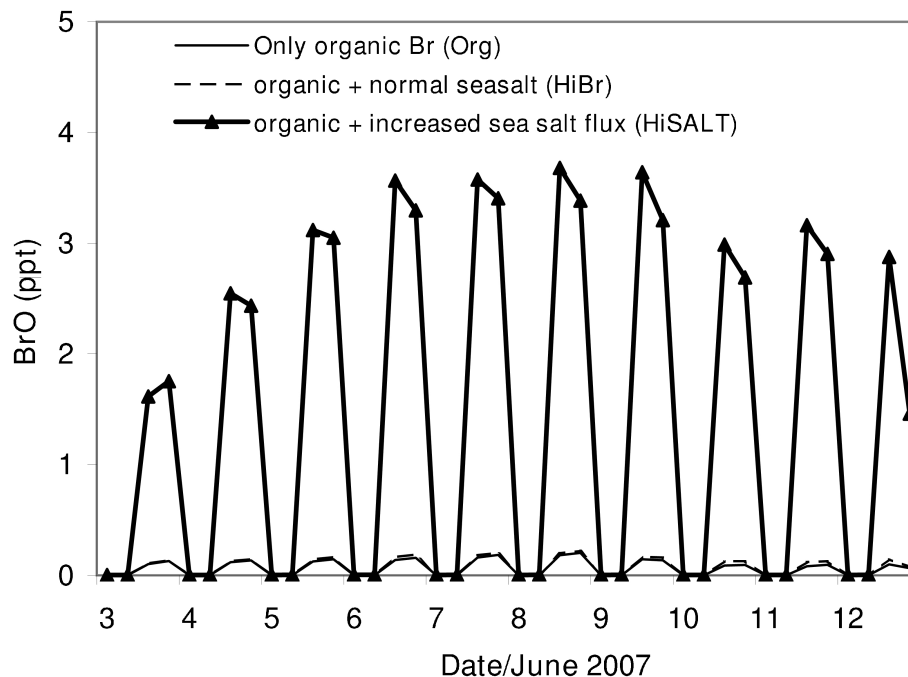


**Fig. 6.** Simulated BrO over Cape Verde, with different bromine sources. The thin solid line represents the model run with bromocarbons only (Org); the dashed line represents the model run with an organic bromine source plus normal sea salt production from the open ocean, calculated by the Monahan et al. (1986) formula (HiBr). The solid line with triangles represents the run with an organic bromine source plus an elevated inorganic source over the region 10–20° N, 20–30° W (HiSALT).

[Title Page](#)[Abstract](#)[Introduction](#)[Conclusions](#)[References](#)[Tables](#)[Figures](#)[◀](#)[▶](#)[◀](#)[▶](#)[Back](#)[Close](#)[Full Screen / Esc](#)[Printer-friendly Version](#)[Interactive Discussion](#)

**Bromocarbons in the  
tropical marine  
boundary layer**

L. M. O'Brien et al.

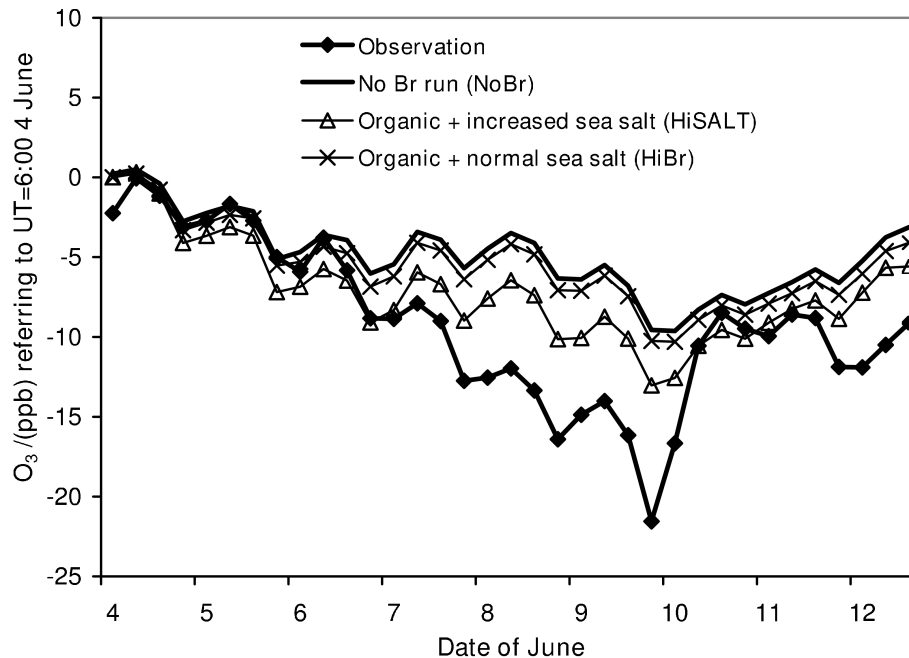


**Fig. 7.** Observed and modelled ozone differences referring to values at UT=06:00 on 4 June. Modelled runs are NoBr, HiBr and HiSALT.

[Title Page](#)[Abstract](#)[Introduction](#)[Conclusions](#)[References](#)[Tables](#)[Figures](#)[◀](#)[▶](#)[◀](#)[▶](#)[Back](#)[Close](#)[Full Screen / Esc](#)[Printer-friendly Version](#)[Interactive Discussion](#)

**Bromocarbons in the  
tropical marine  
boundary layer**

L. M. O'Brien et al.

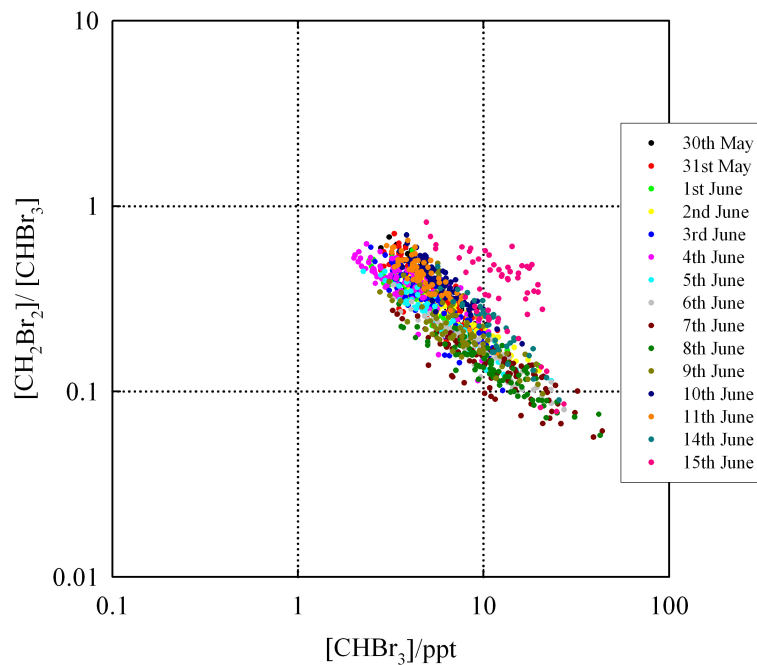


**Fig. 8a.**  $\text{CH}_2\text{Br}_2/\text{CHBr}_3$  plotted against  $[\text{CHBr}_3]$  for all dates, coloured by day, on a log-log scale.

[Title Page](#)[Abstract](#)[Introduction](#)[Conclusions](#)[References](#)[Tables](#)[Figures](#)[◀](#)[▶](#)[◀](#)[▶](#)[Back](#)[Close](#)[Full Screen / Esc](#)[Printer-friendly Version](#)[Interactive Discussion](#)

**Bromocarbons in the  
tropical marine  
boundary layer**

L. M. O'Brien et al.

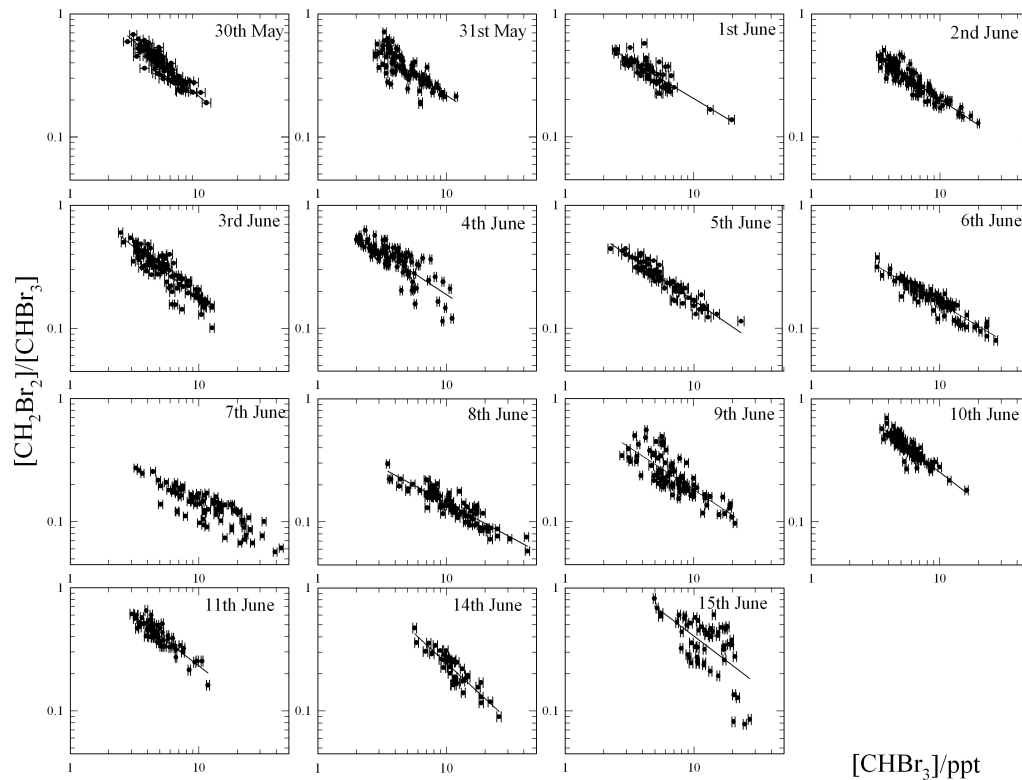


**Fig. 8b.**  $[\text{CH}_2\text{Br}_2]/[\text{CHBr}_3]$  plotted against  $[\text{CHBr}_3]$  for individual days. Plots are shown on a log-log scale.

Title Page

Abstract

Introduction

Conclusions

References

Tables

Figures

◀

▶

◀

▶

Back

Close

Full Screen / Esc

Printer-friendly Version

Interactive Discussion



**Bromocarbons in the  
tropical marine  
boundary layer**

L. M. O'Brien et al.

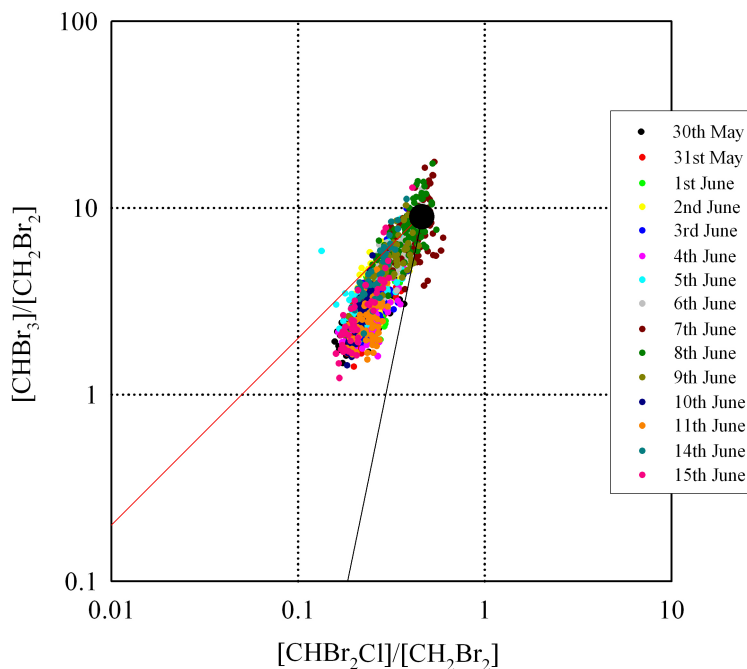


**Fig. 9.** Log-log plots of  $[\text{CHBr}_3]/[\text{CH}_2\text{Br}_2]$  versus  $[\text{CHBr}_2\text{Cl}]/[\text{CH}_2\text{Br}_2]$ , following Yokouchi et al. (2005). All of the data is shown in this plot. The solid red line is the 1:1 dilution line. The solid black line is the chemical decay line, estimated from the lifetime of the 3 species. In this case, we have followed the example of Yokouchi et al. (2005) and used lifetimes of 26 days, 69 days and 120 days respectively for  $\text{CHBr}_3$ ,  $\text{CHBr}_2\text{Cl}$  and  $\text{CH}_2\text{Br}_2$ . Thus the chemical decay line has a slope of 4.89. The large black point near the top of the data set is the estimated emission ratio of the compounds (where ratios are at a maximum), based on 95th percentiles.

[Title Page](#)[Abstract](#)[Introduction](#)[Conclusions](#)[References](#)[Tables](#)[Figures](#)[◀](#)[▶](#)[◀](#)[▶](#)[Back](#)[Close](#)[Full Screen / Esc](#)[Printer-friendly Version](#)[Interactive Discussion](#)

**Bromocarbons in the  
tropical marine  
boundary layer**

L. M. O'Brien et al.

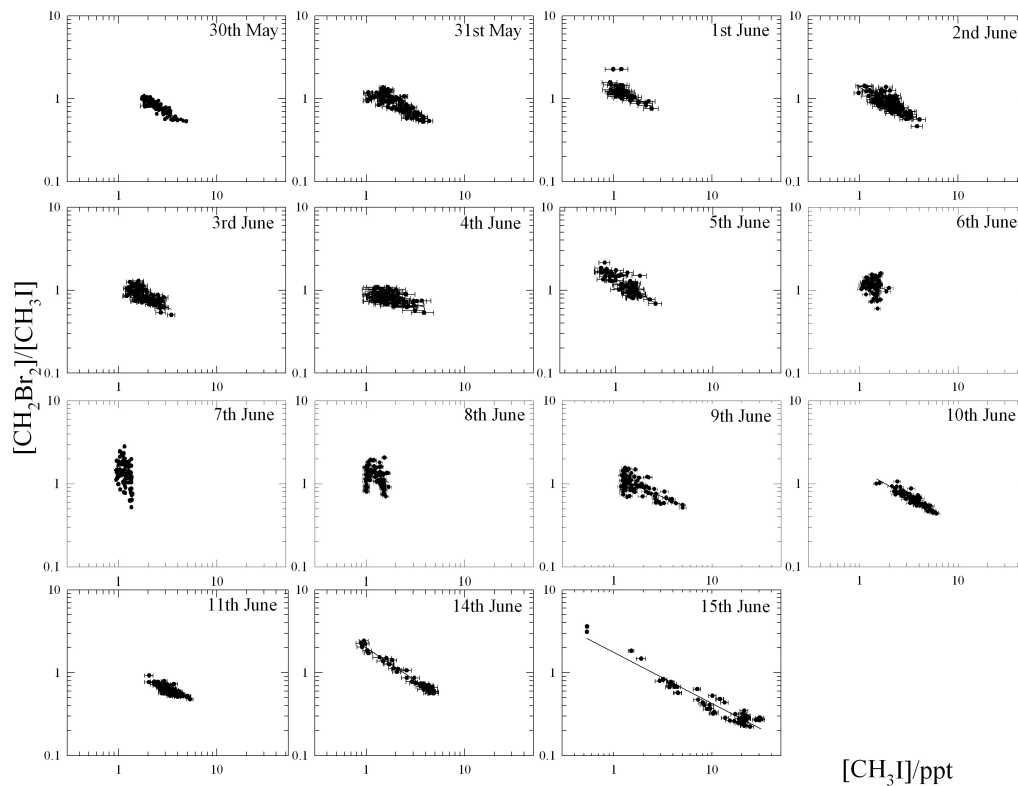


**Fig. 10.**  $[\text{CH}_2\text{Br}_2]/[\text{CH}_3\text{I}]$  plotted against  $[\text{CH}_3\text{I}]$  for individual days. Plots are shown on a log-log scale.

[Title Page](#)[Abstract](#)[Introduction](#)[Conclusions](#)[References](#)[Tables](#)[Figures](#)[◀](#)[▶](#)[◀](#)[▶](#)[Back](#)[Close](#)[Full Screen / Esc](#)[Printer-friendly Version](#)[Interactive Discussion](#)